However, in Task 2, there was only one way to solve the problem. In Task 2, the participants were required to choose one correct answer out of three options. Three different versions of each problem and two control tasks were alternatively presented in a counterbalanced manner. Each subject was instructed to refrain from moving the eyes during tasks and the ocular movement was monitored through the video focusing on the participant's face. The amateurs performed similar tasks with easier contents designed for nonprofessionals. Each task was presented on a screen three times for 90 s. The participants were required to state their answer for each Task 2 problem and assess the difficulty for each Task 1 and Task 2 problem as a visual analog scale (VAS, from the easiest 1 to the most difficult 10) every time after completion of each scan for Task 2. The VAS value for Task 2 was defined as follows: VAS value for Task 2=(individual VAS score in Task 2)/(mean VAS score averaged between Task 1 and Task 2)×100.

2.3. Apparatus and procedure

The experiment was conducted with a brain-purpose high-resolution Hamamatsu Phtonics PET scanner [30] capable of yielding 47-slice images simultaneously with a spatial resolution of 2.9 mm (full width at half maximum) transaxially and 3.0 mm axially and with a 163-mm axial field of view. After a 10-min transmission scan for attenuation correction using a $^{68}Ge/^{68}Ga$ source with the subject's head fixed by a radiosurgery-purpose thermoplastic facemask, a 60-s emission scan was acquired from when the radiotracer first entered the cerebral circulation after intravenous bolus injection of 300 MBq of $H_2^{15}O$ [26]. The timing of the PET start to collect the rising phase of the head curve radioactivity was described previously [16]. After back projection and filtering with a Hanning filter of a cut-off frequency of 0.2 cycles per pixel, image resolution of reconstructed regional cerebral blood flow was 6.0×6.0×3.6 mm full width at half maximum and the voxel size was measured to be 1.3×1.3×3.4 mm.

2.4. Data analysis

The whole-brain CBF data were analyzed using SPM99 software (Wellcome Department of Cognitive Neurology, London, UK, http://www.fil.ion.ucl.ac/spm/spm99.html [9]). The analytic procedure of SPM was basically the same as the methods in our previous reports [16,22]. Briefly, spatially normalized data based on the standard stereotaxic brain atlas [28] after being realigned to the first image data were smoothed by an isotropic Gaussian kernel of 8 mm. The effect of variance from global CBF was excluded by proportional scaling with the global CBF normalized to 50 ml/100g/min. So, the individual rCBF response was regarded as centered adjusted rCBF value. The resultant Z-maps were displayed on the three-dimensional MRI data obtained from all participants prior to each PET session. Between-group comparison was performed using VAS as a covariate because the difficulty of go problems presented was different from each group. In correlation analyses, the ranks in professional go players were used as covariates for testing the judgment process at different stages (both Task 1 and Task 2). Significant differences in CBF between conditions were estimated with a statistical threshold set at $p<0.05$ corrected for multiple comparisons at voxel levels. In the SPM correlation analysis, statistical significance was given as $p<0.001$, uncorrected.

3. Results

3.1. Performance

There was no significant difference in VAS for task difficulty between groups. However, amateurs less frequently

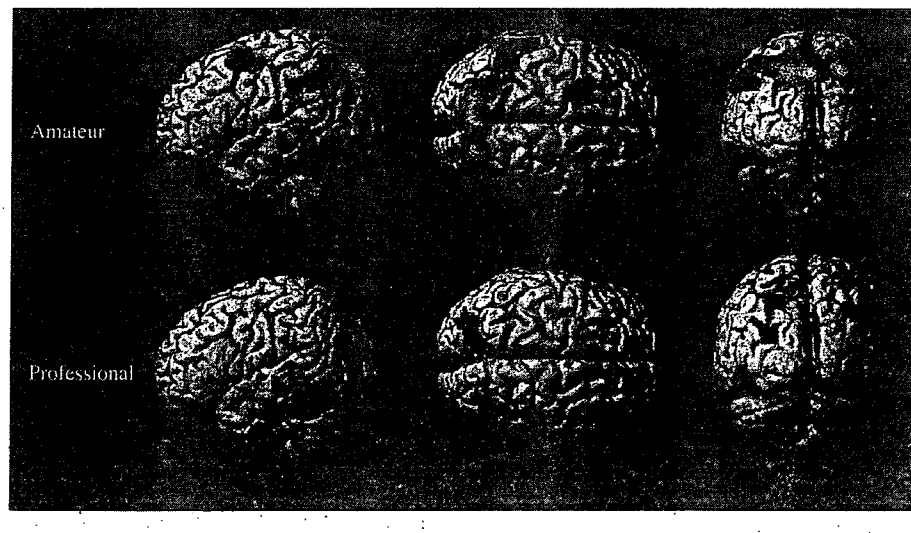

Fig. 2. Brain activation during opening stage thinking (green) (Task 1 vs. Base) and the life-or-death judgment (red) (Task 2 vs. Base) irrespective of answer content in the amateur and professional go groups ($p<0.05$, corrected). Top row: amateur, bottom row: professional. Yellow denotes an overlap of green and red areas.

Table 1
Activated brain regions in checkmate decision with and without correct answers relative to the baseline condition in professional and amateur go players

Group	Activated area	BA	Coordinates ($x\ y\ z$)	Z score
Successful response				
Professional	L precuneus	7	−12 −78 50	4.62
	R precuneus	7	18 −78 54	4.22
	R cerebellum (posterior lobe)	–	26 −44 −46	4.01
Amateur	Precuneus	7	0 −76 52	5.32
	R intraparietal sulcus	40/7	50 −44 42	4.98
	L precuneus	7	−16 −76 50	4.66
Failed response				
Professional	L supramarginal cortex	40	−60 −38 46	5.71
	R supramarginal cortex	40	60 −42 42	5.23
Amateur	R intraparietal sulcus	40/7	42 −52 44	6.60
	R precuneus	7	2 −76 48	6.27
	L intraparietal sulcus	40/7	−30 −60 48	5.94
	R superior precentral sulcus	6	30 −2 58	5.73
	L superior precentral sulcus	6	−24 6 58	5.39
	R middle temporal gyrus	19	42 −80 20	5.37
	L precuneus	7	−16 −72 50	5.32
	L supramarginal cortex	40	−50 −50 40	5.18

BA: Brodmann area, R: right, L: left.

made correct answers than professionals ($p<0.05$, χ^2 test) (Fig. 1B). The video showed various degrees of the eye blink and minimal eye movement during each scan in all participants, indicating that the present finding could eliminate the effect of saccadic eye movement. No motor behavior was found during scans in all subjects.

Table 2
Brain regions significantly activated during judging correctly in two groups

Group	Activated area	BA	Coordinates ($x\ y\ z$)	Z score
Professional	R cerebellum (anterior lobe)	–	20 −74 −18	4.73
	L cerebellum (anterior lobe)	–	−24 −76 −14	4.43
	L precuneus	7	−18 −66 60	4.36
	R cerebellum (posterior lobe)	–	36 −48 −36	4.29
Amateur	L superior precentral sulcus	6	−22 0 60	4.87
	R cuneus	17	14 −102 0	4.60
	L supramarginal cortex	40	−60 −28 40	4.53
	L superior precentral sulcus	6	26 0 64	4.51

BA: Brodmann area, R: right, L: left.

3.2. PET results

Within-subject subtraction analysis irrespective of outcome (correct or false answer) showed extensive activations in the parietal and prefrontal cortices and cerebellum bilaterally in amateur go players in either type of task (upper images, Fig. 2), whereas more focal activated regions were observed in the parietal and temporooccipital cortices and right cerebellum in the professional group (bottom images, Fig. 2). When the players made correct answers in Task 2 (checkmate judgment), the bilateral superior parietal cortices (precuneus) and the right cerebellum was activated in the professional group, and the precuneus and intraparietal sulcus region were significantly activated in amateurs (Table 1, Fig. 3, green). When thinking incorrectly, the bilateral supramarginal cortices were activated in the professional group, and the broader cortical regions covering the premotor and parietal cortices bilaterally were activated in the amateur group (Table 1, Fig. 3, red).

In the checkmate judgment process with correct response, the precuneus and cerebellar cortex were more

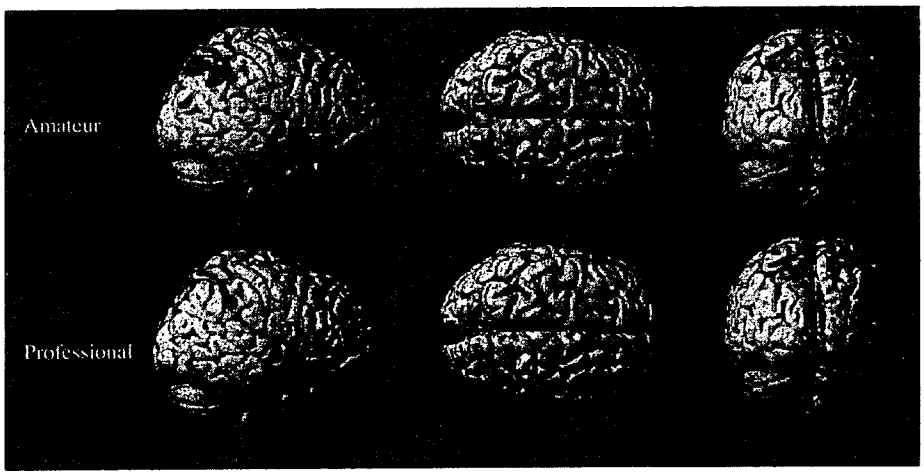

Fig. 3. Brain activation during the life-or-death deliberation with (green) and without (red) correct answers in the amateur and professional go groups ($p<0.05$, corrected). Top row: amateur, bottom row: professional. Yellow denotes an overlap of green and red areas.

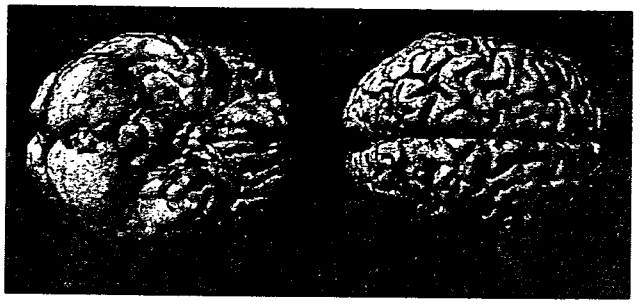

Fig. 4. Brain regions more activated during the life-or-death deliberation with correct reply in the professional than amateur group (green), and more activated in the amateur than professional group (red) ($p<0.05$, corrected).

strongly activated in the professional group, while the premotor and parietooccipital activation were stronger in the amateur group (Table 2, Fig. 4). Scattered plotting revealed that the CBF increase in the left premotor cortex correlated significantly with the task difficulty (VAS) in the amateur group (Fig. 5A, $p<0.05$, $r=0.62$), whereas the right cerebellar CBF increase correlated with the score in the professional group (Fig. 5B, $p<0.05$, $r=0.61$).

Correlation analysis in the professional group showed that the bilateral cerebellum in territorial planning (Task 1) and the right cerebellum in checkmate-decision (Task 2) correlated positively with professional ranks (Fig. 6, $p<0.001$, uncorrected).

4. Discussion

The present study revealed different neural substrates involved in cognitive processes between professional and amateur go players (irrespective of successful or failed outcome during the go game). The precuneus and cerebellum were engaged more in the checkmate judgment process in professional players, while the premotor and occipitoparietal cortices were remarkably activated in amateurs. Although unsuccessful performance caused broader brain activation during the checkmate judgment in the amateur group (Fig. 3), only focal regions were detected in the professional group, suggesting more economical use of the brain energy in professional go players. As suggested in a recent study of professional musicians [17], the different cortical representations in judgment process could be interpreted as a result of cortical plasticity in highly skilled go players.

In view of correct or incorrect responses during the game, it was found that the precuneus was significantly activated during the checkmate judgment with correct answers in both professional and amateur players. This region connects to the anterior cingulate, prefrontal, lateral parietal and temporal cortices [29]. This anatomical connection suggests that the precuneus plays a role in orchestrating multimodal associative functions. Hence, almost all the participants, when performing successfully, would have utilized every part region of the brain related to the precuneus activity. It has been reported that the precuneus is activated more during silent tasks for motor imagery [4,24] and during motor imagery of complete finger movement than during explicit execution [11]. Thus, it is suggested that the precuneus might allow complete mental reproduction of the configuration of go stones on the imagined board in the players with correct responses. The left precuneus was engaged in this strategic thinking in professional players. Therefore, one can assume that professional go players exploit this ability efficiently and make the most of the motor imagery skills through highly vigilant or conscious retrieval of acquired memory [2]. In contrast, unsuccessful deliberation caused supramarginal activation in professionals and the prefrontal-temporoparietal activation in amateurs. A recent fMRI study showed that the supramarginal cortex might be involved in an enactment effect that improves performance encoding ability [27]. This suggests that trial and error of different

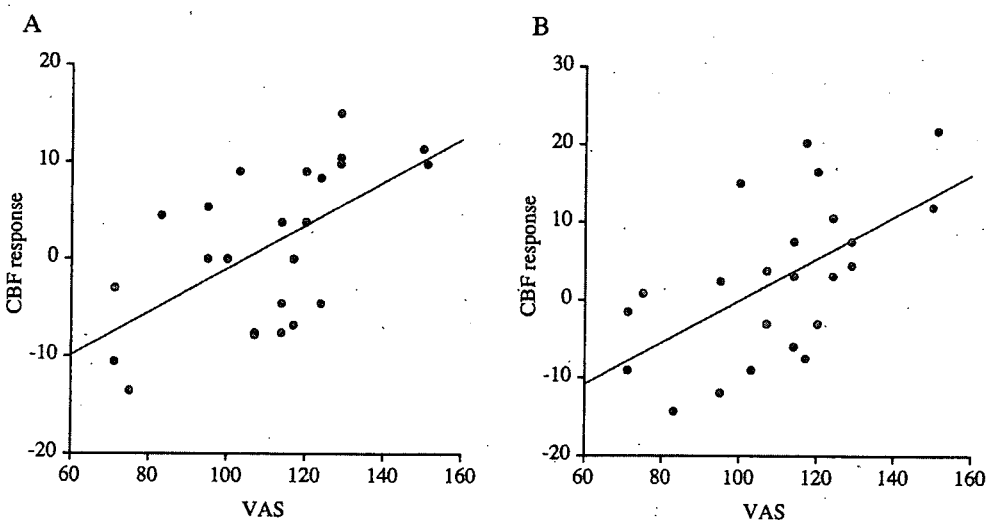

Fig. 5. Correlation analyses between VAS scores (%) and premotor CBF responses (%) in the amateur group (A) and between VAS scores and cerebellar CBF responses in the professional group (B).

Fig. 6. Activated brain regions significantly correlated with professional "dan" ranks during the territorial planning (red) and the life-or-death judgment (green) in the professional group ($p<0.001$, uncorrected).

moves might have activated the supramarginal cortex in professional players. In contrast with the professional go players, amateur players lacking in strategic or enactment ability required incorporation of the prefrontal (premotor) and parietooccipital cortex, including the precuneus, to solve the problem (Fig. 4). This premotor activity was positively associated with the difficulty of the go problem (Fig. 5A). This pattern of activation in amateurs is consistent with the activation results in a recent fMRI study showing that the premotor and precuneus regions were activated conjointly during visuomotor operation [13] and in a chess study revealing activations of the superior frontal and occipitoparietal regions during checkmate judgment [21]. The difference of these patterns in judgment processes between professional and amateur go players may reflect a distinctive professional way of thinking leading to greater efficiency, which requires a smaller number of active neurons in specific regions incorporated in the critical situations during the go game.

Another interesting result from the comparison of the professional and amateur group in the present study was that the cerebellum was more engaged in the endgame strategy in professional players. The cerebellum has been implicated in motor imagery [8,19] and problem solving [18] in nonmotor cognitive operations. As the rank of professional go players became higher, this cerebellar cortex was more activated as shown in Fig. 6. In addition, this cerebellar activity correlated positively with VAS for task difficulty (Fig. 5B). This seemingly contradictory finding suggests that VAS of professionals in the present study might indicate uneasy emotion, because the cerebellar activation was correlated with gradual increase in task-demand during mental rehearsal [3]. Actually, some higher ranking professionals exhibited high VAS scores and excellent achievement. Thus, the cerebellum in the professional players might be associated with predictive control that guides online imagery motor performance during tense situations of the go game.

There are a few methodological caveats that have to be taken into account for the present study. The task contents in life-or-death problems given to amateurs were different from those given to professionals because amateurs would not have been able to solve the difficult tasks given to the professionals. Although the VAS for task difficulty was found similar between the groups, the strategy to solve the problem might be different. The present study did not attempt to elucidate each step of problem solving or strategic cognitive processes. This issue may be important for unraveling the mystery of the expert's mind. The questionnaire after each session of PET scans revealed that some professionals had solved the problems early within the 60-s period and spent the remaining times verifying the answer. This might cause not only weaker activation of brain region responsible for the execution of solving tasks, but also incorporation of brain regions irrelevant to the judgment process. Thus, the present result might reflect the summation of neural substrates for judgment and imagery retrieval processes occurring in the professional mind.

In summary, our results have shown that the professional judgment requires the precuneus and cerebellar activations during the go game. This suggests that visual imagery and motor imagination may be important for the highly skilled tactics of professionals. In contrast, it seems that the extensive frontoparietal regions functioning partly in visuomotor processing operate dominantly in execution of solving problems in amateur go players. In view of brain rehabilitation for the elderly and patients with dementia, playing a game of go may cause premotor activation, which may be of great value for stimulating the brain, because incorporation of the premotor region activity is necessary for executing arithmetic cognitive tasks in Alzheimer's disease patients [23]. The different pattern of cognitive processes between expert and amateur go players may reflect the brain functional plasticity or functional specialization that is acquired later in domain-specific experts.

Acknowledgments

We would like to thank Mr. Zenta Takekawa (Japan Go Association) for his task selection, Mr. Fumitoshi Nakamura and the staff of the Japan Go Association for their constant support in the present study.

References

[1] G. Allen, R.B. Buxton, E.C. Wong, et al., Attentional activation of the cerebellum independent of motor involvement, Science 275 (1997) 1940–1943.

[2] N.C. Andreasen, D.S. O'Leary, S. Paradiso, et al., The cerebellum plays a role in conscious episodic memory retrieval, Hum. Brain Mapp. 8 (1999) 226–234.

[3] H. Boecker, A.O. Ceballos-Baumann, P. Bartenstein, et al., A H(2)(15)O positron emission tomography study on mental imagery of movement sequences—the effect of modulating sequence length and direction, Neuroimage 17 (2002) 999–1009.

[4] E. Bonda, M. Petrides, S. Frey, Neural correlates of mental transformations of the body-in-space, Proc. Natl. Acad. Sci. U. S. A. 92 (1995) 11180–11184.

[5] C. Calarge, N.C. Andreasen, D.S. O'Leary, Visualizing how one brain understands another: a PET study of theory of mind, Am. J. Psychiatry 160 (2003) 1954–1964.

[6] X. Chen, D. Zhang, X. Zhang, et al., A functional MRI study of high-level cognition: II. The game of GO, Brain Res. Cogn. Brain Res. 16 (2003) 32–37.

[7] C. Cho, Go: A Complete Introduction of the Game, Kiseido Publishing, Tokyo, 1997, 1–138 pp.

[8] J. Decety, H. Sjoholm, E. Ryding, et al., Cerebellum participates in mental activity: tomographic measurements of regional cerebral blood flow, Brain Res. 535 (1990) 313–317.

[9] K.J. Friston, A.P. Holmes, K.J. Worsley, et al., Statistical parametric mapping in functional imaging: a general linear approach, Hum. Brain Mapp. 2 (1995) 189–210.

[10] J.H. Gao, L.M. Parsons, J.M. Bower, et al., Cerebellum implicated in sensory acquisition and discrimination rather than motor control, Science 272 (1996) 545–547.

[11] E. Gerardin, A. Sirigu, S. Lehericy, et al., Partially overlapping neural networks for real and imagined hand movements, Cereb. Cortex 10 (2000) 1093–1104.

[12] J. Grezes, J. Decety, Does visual perception of object afford action? Evidence from a neuroimaging study, Neuropsychologia 40 (2002) 212–222.

[13] T. Hanakawa, M. Honda, T. Okada, et al., Neural correlates underlying mental calculation in abacus experts: a functional magnetic resonance imaging study, Neuroimage 19 (2003) 296–307.

[14] T. Hatta, T. Kogure, A. Kawakami, Hemisphere specialization of Go experts in visuospatial processing, Am. J. Psychol. 112 (1999) 571–584.

[15] M. Ito, Movement and thought: identical control mechanisms by the cerebellum, Trends Neurosci. 16 (1993) 448–450.

[16] M. Iwase, Y. Ouchi, H. Okada, et al., Neural substrates of human facial expression of pleasant emotion induced by comic films: a PET Study, Neuroimage 17 (2002) 758–768.

[17] L. Jancke, N.J. Shah, M. Peters, Cortical activations in primary and secondary motor areas for complex bimanual movements in professional pianists, Brain Res. Cogn. Brain Res. 10 (2000) 177–183.

[18] S.G. Kim, K. Ugurbil, P.L. Strick, Activation of a cerebellar output nucleus during cognitive processing, Science 265 (1994) 949–951.

[19] A.R. Luft, M. Skalej, A. Stefanou, et al., Comparing motion- and imagery-related activation in the human cerebellum: a functional MRI study, Hum. Brain Mapp. 6 (1998) 105–113.

[20] E.A. Maguire, R.S. Frackowiak, C.D. Frith, Recalling routes around London: activation of the right hippocampus in taxi drivers, J. Neurosci. 17 (1997) 7103–7110.

[21] P. Nichelli, J. Grafman, P. Pietrini, et al., Brain activity in chess playing, Nature 369 (1994) 191.

[22] Y. Ouchi, H. Okada, E. Yoshikawa, et al., Brain activation during maintenance of standing postures in humans, Brain 122 (1999) 329–338.

[23] Y. Ouchi, E. Yoshikawa, M. Futatsubashi, et al., Activation in the premotor cortex during mental calculation in patients with Alzheimer's disease: relevance of reduction in posterior cingulate metabolism, Neuroimage 22 (2004) 155–163.

[24] L.M. Parsons, P.T. Fox, J.H. Downs, et al., Use of implicit motor imagery for visual shape discrimination as revealed by PET, Nature 375 (1995) 54–58.

[25] M. Pesenti, L. Zago, F. Crivello, et al., Mental calculation in a prodigy is sustained by right prefrontal and medial temporal areas, Nat. Neurosci. 4 (2001) 103–107.

[26] M.E. Raichle, W.E.W. Martin, P. Herscovitch, et al., Brain blood flow measured with intravenous H2(15)O: II. Implementation and validation, J. Nucl. Med. 24 (1983) 790–798.

[27] M.O. Russ, W. Mack, C.R. Grama, et al., Enactment effect in memory: evidence concerning the function of the supramarginal gyrus, Exp. Brain Res. 149 (2003) 497–504.

[28] J. Talairach, P. Tournoux, Co-planer Stereotaxic Atlas of the Human Brain: 3-Dimensional Proportional System: An Approach to Cerebral Imaging, Georg Thieme, Stuttgart, 1988.

[29] E.P.M. Vianna, G. Van Hoesen, J. Parvizi, Efferent connections of the primate posterior cingulate, retrosplenial and mesial parietal cortices, J. Neurosci. 587 (2002) 12.

[30] M. Watanabe, K. Shimizu, T. Omura, et al., A new high resolution PET scanner dedicated to brain research, IEEE Trans. Nucl. Sci. 49 (2002) 634–639.

Brain Serotonin Transporter Density and Aggression in Abstinent Methamphetamine Abusers

Yoshimoto Sekine, MD, PhD; Yasuomi Ouchi, MD, PhD; Nori Takei, MD, PhD, MSc; Etsuji Yoshikawa, BA; Kazuhiko Nakamura, MD, PhD; Masami Futatsubashi, BA; Hiroyuki Okada, BA; Yoshio Minabe, MD, PhD; Katsuaki Suzuki, MD, PhD; Yasuhide Iwata, MD, PhD; Kenji J. Tsuchiya, MD; Hideo Tsukada, PhD; Masaomi Iyo, MD, PhD; Norio Mori, MD, PhD

Context: In animals, methamphetamine is known to have a neurotoxic effect on serotonin neurons, which have been implicated in the regulation of mood, anxiety, and aggression. It remains unknown whether methamphetamine damages serotonin neurons in humans.

Objective: To investigate the status of brain serotonin neurons and their possible relationship with clinical characteristics in currently abstinent methamphetamine abusers.

Design: Case-control analysis.

Setting: A hospital research center.

Participants: Twelve currently abstinent former methamphetamine abusers (5 women and 7 men) and 12 age-, sex-, and education-matched control subjects recruited from the community.

Interventions: The brain regional density of the serotonin transporter, a structural component of serotonin neurons, was estimated using positron emission tomography and *trans*-1,2,3,5,6,10-beta-hexahydro-6-[4-(methylthio) phenyl]pyrrolo-[2,1-a]isoquinoline ([^{11}C](+)McN-5652). Estimates were derived from region-of-interest and statistical parametric mapping methods, followed by within-case analysis using the measures of clinical variables.

Main Outcome Measures: The duration of methamphetamine use, the magnitude of aggression and depressive symptoms, and changes in serotonin transporter density represented by the [^{11}C](+)McN-5652 distribution volume.

Results: Methamphetamine abusers showed increased levels of aggression compared with controls. Region-of-interest and statistical parametric mapping analyses revealed that the serotonin transporter density in global brain regions (eg, the midbrain, thalamus, caudate, putamen, cerebral cortex, and cerebellum) was significantly lower in methamphetamine abusers than in control subjects, and this reduction was significantly inversely correlated with the duration of methamphetamine use. Furthermore, statistical parametric mapping analyses indicated that the density in the orbitofrontal, temporal, and anterior cingulate areas was closely associated with the magnitude of aggression in methamphetamine abusers.

Conclusions: Protracted abuse of methamphetamine may reduce the density of the serotonin transporter in the brain, leading to elevated aggression, even in currently abstinent abusers.

Arch Gen Psychiatry. 2006;63:90-100

Author Affiliations: Department of Psychiatry and Neurology, Hamamatsu University School of Medicine, Hamamatsu, Japan (Drs Sekine, Takei, Nakamura, Minabe, Suzuki, Iwata, Tsuchiya, and Mori); Positron Medical Center, Hamamatsu Medical Center, Hamakita, Japan (Dr Ouchi); Division of Psychological Medicine, Institute of Psychiatry, London, England (Dr Takei); Central Research Laboratory, Hamamatsu Photonics KK, Hamakita (Dr Tsukada and Messrs Yoshikawa, Futatsubashi, and Okada); and Department of Psychiatry, Chiba University Graduate School of Medicine, Chiba, Japan (Dr Iyo).

METHAMPHETAMINE IS A powerfully addictive drug, and the number of its abusers has been steadily increasing worldwide.[1-5] Long-term methamphetamine abuse can produce various psychiatric symptoms, including psychosis, depression, anxiety, and aggression, under conditions of intoxication and withdrawal.[6,7] These psychiatric states are sometimes prolonged, in the form of residual symptoms, and are easily exacerbated in some long-term abusers by methamphetamine reuse or by psychological stress.[3,8-10]

In animal studies, the biochemical effects of the neurotoxicity of methamphetamine on mature neurons, especially on the dopaminergic and serotonergic axon arbors, are well documented,[11,12] although neurotoxic methamphetamine may also cause cell death through apoptosis or necrosis.[12,13] However, methamphetamine-induced neuronal damage is thought to vary across species.[14,15] For example, in contrast to the findings in rats,[11] which indicate that serotonergic neurons are more sensitive to the methamphetamine-induced toxicity than are dopaminergic neurons, recent findings[16] have suggested that serotonergic neurons in nonhuman primates seem to be less affected by methamphetamine administration than are dopaminergic neurons.

In vivo studies using positron emission tomography (PET) are helpful for understanding the contribution of methamphetamine neurotoxicity and induced

Table 1. Demographic and Clinical Characteristics of the 24 Study Participants

	Control Subjects (n = 12)		Methamphetamine Abusers (n = 12)*	
	Mean ± SD	Range	Mean ± SD	Range
Age, y	31.8 ± 6.6	21-44	31.4 ± 6.8	21-44
Education, y	11.5 ± 1.2	9-12	11.1 ± 2.1	9-12
Duration of methamphetamine use, y	NA	NA	6.7 ± 3.2	1.5-11.0
Duration of methamphetamine abstinence, y	NA	NA	1.6 ± 1.3	0.5-5.0
BPRS positive symptoms subscale score	NA	NA	5.3 ± 3.9	0-14
BPRS negative symptoms subscale score	NA	NA	0.0 ± 0.0	0.0
17-Item HAM-A score	NA	NA	3.8 ± 6.3	0-16
17-Item HAM-D score	NA	NA	4.0 ± 6.3	0-19
Scale for methamphetamine craving score	NA	NA	4.9 ± 3.4	1-10
Aggression Questionnaire score†	30.2 ± 1.7	29-34	75.0 ± 13.9‡	46-97

Abbreviations: BPRS, Brief Psychiatric Rating Scale; HAM-A, Hamilton Rating Scale for Anxiety; HAM-D, Hamilton Rating Scale for Depression; NA, not applicable.
*All the abusers took methamphetamine intravenously.
†Higher scores represent greater aggression.
‡Significantly difference from control subjects using the *t* test ($P<.001$).

neural damage to the long-term withdrawal syndrome. Recent PET studies have shown that long-term use of methamphetamine decreases the density of DA transporters, which are located on dopaminergic terminals in the human brain[1-3,17,18]; moreover, long-term use of methamphetamine may cause severe positive symptoms (eg, delusions and hallucinations) and an increased reduction in DA transporter density.[3,18] However, to date, no studies have addressed the alteration of serotonergic neurons in methamphetamine abusers. In addition, it is not known whether such changes, if found, could be related to the psychiatric symptoms frequently observed in currently abstinent methamphetamine abusers.

We, therefore, examined the possibility of changes in the density of the serotonin transporter, an index of serotonin neuronal damage,[19-25] in methamphetamine abusers by means of PET. This information was then considered as part of an evaluation of the potential associations between serotonin transporter density and participant clinical characteristics.

METHODS

PARTICIPANTS

The ethics committees of the Hamamatsu University School of Medicine and Hamamatsu Medical Center approved this study. Written informed consent was obtained from each participant after they were provided an explanation of the study procedures. Twelve currently abstinent methamphetamine abusers who had previously abused only methamphetamine (ie, monodrug abusers) and 12 age-, sex-, and education-matched control subjects participated in this study (**Table 1**). Potential participants were recruited from the community by means of poster advertisements and word of mouth in and around Hamamatsu City, which is located in the middle of the mainland of Japan. The participants in the methamphetamine group were required to attend a weekly meeting at the Drug Detoxification and Rehabilitation Program Center of Hattori Mental Hospital (Iwata, Japan) to maintain and ensure abstinence until the PET study was conducted.

All the methamphetamine abusers had used the drug recreationally and had no history of toxic or high-dose methamphetamine use. None of the abusers had any history of hospitalization or treatment at psychiatric hospitals. We assessed the participants regarding the use of other illicit drugs, including (±)3,4-methylenedioxymethamphetamine, cocaine, cannabis, heroin, and toluene, because these substances are known to cause psychiatric symptoms and to affect neural transmission in the brain.[19,26,27] However, none of the methamphetamine abusers recruited for the present study were found to have a history of such illicit drug use. All the methamphetamine abusers were naive to neuropsychiatric medications, such as antipsychotics and antidepressants. None of the methamphetamine abusers had a history of psychiatric disorders, including antisocial or intermittent explosive disorder, or a history of increased aggression before the use of methamphetamine. The controls were healthy and had never used methamphetamine or any other illicit drugs, and none of them met any of the relevant criteria according to the *Diagnostic and Statistical Manual of Mental Disorders, Fourth Edition*.[28] The control and methamphetamine groups showed similar habits of occasional drinking and smoking, but none of the participants fulfilled either the alcohol- or the nicotine-related *Diagnostic and Statistical Manual of Mental Disorders, Fourth Edition* criteria. These evaluations were determined using the Structured Clinical Interview for the *Diagnostic and Statistical Manual of Mental Disorders, Fourth Edition*.[29] To increase the accuracy of the abusers' profiles, detailed information on the duration of methamphetamine use and the history of psychiatric symptoms was retrospectively obtained using Structured Clinical Interview for the *Diagnostic and Statistical Manual of Mental Disorders, Fourth Edition*–based interviews with the abusers and their family members. The period of methamphetamine use was defined as the duration between the first and last use. When intervals of abstinence longer than 1 month occurred during the duration of methamphetamine use as defined, these intervals were subtracted from the total duration value. The methamphetamine abstinence period was arbitrarily defined as the duration between the day of the last use of methamphetamine and that of the PET examination.

DRUG SCREENING

During the weekly meeting at the Drug Detoxification and Rehabilitation Program Center, the absence of recent methamphetamine and other drug use was regularly confirmed using a rapid

immunoassay for the qualitative detection of the metabolites of the following 8 classes of drugs: amphetamines, including methamphetamine and (±)3,4-methylenedioxymethamphetamine; barbiturates; benzodiazepines; cocaine; methadone; opiates; tetrahydrocannabinol; and tricyclic antidepressants (Triage8; Biosite Diagnostics, San Diego, Calif). In addition, the participants were tested for urinary hippuric acid, a biomarker of toluene use, using high-performance liquid chromatography according to the standard diagnostic methods.[27] These assessments were also performed on the same day as the PET examination. When necessary, we assessed hair samples using high-performance liquid chromatography, which enabled us to verify long periods of methamphetamine abstinence.[30]

CLINICAL EVALUATION

The severity of psychiatric symptoms in methamphetamine abusers was evaluated using the Aggression Questionnaire (AQ)[31]; the scores can range from 29 to 145, with higher scores representing greater aggression. In addition, the 17-item Hamilton Rating Scale for Anxiety,[32] the 17-item Hamilton Rating Scale for Depression,[33] and positive and negative symptom subscores[34] on the Brief Psychiatric Rating Scale[35] were included in the evaluation. The Subjective Drug Effect Rating Scale for Cocaine[36] was modified and used for the assessment of cravings for methamphetamine. The scores on this assessment can range from 1 to 10, with higher scores representing more intense craving sensations (Table 1). These evaluations were performed on the day of the PET examination by a trained research psychiatrist masked to the PET results.

MAGNETIC RESONANCE IMAGING AND MAGNETIC RESONANCE IMAGING–TO-PET COORDINATE PROCEDURES

Three-dimensional magnetic resonance imaging (MRI) was performed just before the PET examination using a 0.3-T MRI unit (MRP7000AD; Hitachi Medical Corp, Tokyo, Japan) and the following acquisition parameters: repetition time, 200 milliseconds; echo time, 23 milliseconds; flip angle, 75°; slice thickness, 2 mm with no gap; and matrix, 256 × 256. In reference to the measurements of the tilt angle and spatial coordinates obtained in the procedure for determining the anterior-posterior intercommissural line on each participant's sagittal MRIs, a PET gantry was set parallel to the anterior-posterior intercommissural line by tilting and moving the gantry for each participant, which permitted reconstruction of the PET images parallel to the anterior-posterior intercommissural line without reslicing; using this approach, we allocated regions of interest (ROIs) on the target areas of the original PET images.[37]

PET PROCEDURES

We used a high-resolution brain PET scanner (model SHR12000; Hamamatsu Photonics KK, Hamamatsu, Japan), which was capable of yielding 47 PET images simultaneously.[38] Before dynamic scanning, a 20-minute transmission scan was performed for attenuation correction using a germanium Ge 68/gallium Ga 68 source with the participant's head fixed by means of a radiosurgery-purpose thermoplastic face mask. Then, after a bolus intravenous injection of a 370-MBq dose of *trans*-1,2,3,5,6,10-beta-hexahydro-6-[4-(methylthio)phenyl]pyrrolo-[2,1-a]isoquinoline ([^{11}C](+)McN-5652), a ligand with high specificity to serotonin transporter,[21,39] 38 serial PET scans (time frames: 4 × 60, 20 × 120, and 14 × 300 seconds) were performed for 92 minutes. A total of 23 arterial blood samples were collected at intervals of 10 seconds to 15 minutes after the tracer injection. The blood samples were analyzed using thin-layer chromatography (Whatman AL SIL G/UV 20 × 20 cm; Whatman Japan KK, Tokyo) and a storage phosphorscreen bioimaging analyzer (model BAS-1500; Fuji Photo Film Co, Tokyo) to determine the levels of unmetabolized tracer.

IMAGE ANALYSIS AND KINETIC MODELING

At the beginning of the study, the MRI voxel size was adjusted to the PET voxel size 3-dimensionally using image processing software (DrView; Asahi Kasei Co, Tokyo) on a Sun workstation (HyperSPARC ss-20; Sun Microsystems, Santa Clara, Calif). These reformatted MRIs with 3-dimensional scales and coordinates identical to those of the PET images were used as anatomic landmarks for the ROI setting, which allowed for minimization of the partial volume effects.[3,18,40,41] An investigator masked to the participant's condition placed 10 ROIs bilaterally over the midbrain, thalamus, caudate nucleus, putamen, amygdala, anterior cingulate cortex, dorsolateral prefrontal cortex, orbitofrontal cortex, temporal cortex, and cerebellar cortex on the MRIs, as previously described.[40,42,43] After delineation of the ROIs was completed on the reformatted MRIs, the PET images were displayed side-by-side with the MRIs. Then, the determined ROIs were placed on the same area on the MRIs and the corresponding PET images.

To assess the brain serotonin transporter density, we analyzed the [^{11}C](+)McN-5652 binding data on the basis of a model that described the radioligand kinetics using a single-tissue compartment and 3 parameters—uptake of radioligand in brain tissue (K_1), release of radioligand from brain tissue (k_2), and blood volume—because the regional brain [^{11}C](+)McN-5652 distribution volume (DV) (ie, the ratio of K_1/k_2) estimated by this model is known to correlate with the known regional brain serotonin transporter density[21,39,44] and has been reported to be suitable for evaluating amphetamine-induced serotonergic neurotoxicity.[21] Cerebral radioactivity was corrected for the contribution of plasma radioactivity, assuming a 5% blood volume in the ROIs. The K_1 and k_2 values were estimated by fitting the metabolite-corrected plasma time–radioactivity curves and the blood volume–corrected brain time–radioactivity curves using a nonlinear least squares algorithm.[3,18,40]

STATISTICAL ANALYSIS

In addition to the ROI method described in the "Methods" section, we also performed a voxel-based whole-brain analysis using statistical parametric mapping (SPM) software (SPM99; Wellcome Department of Cognitive Neurology, Institute of Neurology, London). Based on the same kinetic model as that used for the ROI method, absolute parametric [^{11}C](+)McN-5652 DV images were generated for each participant using biomedical image quantification and kinetic modeling software (PMOD version 2.5; PMOD Technologies Ltd, Zurich, Switzerland) (**Figure 1**).[45,46] To normalize the absolute DV image to the standard stereotaxic brain atlas,[47] we used transformation parameters for early integrated images of [^{11}C](+)McN-5652 (0-20 minutes after injection).[48,49] Subsequently, *t* statistics were performed on a voxel-by-voxel basis (voxel size: 2.0 × 2.0 × 2.0 mm), resulting in *t* statistic maps. Then, the results were transformed to the unit normal distribution. For the SPM analysis, we assessed both group differences in the regional [^{11}C](+)McN-5652 DVs and the possible relationship between the regional changes in [^{11}C](+)McN-5652 DVs and the severity of clinical symptoms in methamphetamine abusers. Age and sex were treated as covariates, and the scores on the clinical measures (AQ, Hamilton Rating Scale for Anxiety, Hamilton Rating Scale for Depression, positive and negative symptoms on

the Brief Psychiatric Rating Scale, and the scale for methamphetamine craving) were considered to be variables of interest. To test hypotheses about the regional specific effects of these variables, the estimates were compared using 2 linear contrasts (positive or negative correlation). According to recently published PET studies[6,50] of methamphetamine abusers, the level of significance was determined using a voxel height threshold of $P=.05$ (corrected). The cluster significance threshold was also set at $P=.05$ (corrected).

To compare the mean values of the demographic and clinical variables in control subjects and methamphetamine abusers, an unpaired t test was used. We tested the main effect of methamphetamine use on [^{11}C](+)McN-5652 DVs derived from 10 brain regions using multivariate analysis of variance. Statistical significance was set at $P<.05$. To investigate the correlation between the [^{11}C](+)McN-5652 DV and the clinical variables in methamphetamine abusers, including the duration of methamphetamine use and abstinence, the Pearson correlation coefficient was computed, with age and sex adjusted for; after applying the Bonferroni correction, the level of statistical significance was set at $P=.005$ (SPSS version 11.0J; SPSS Japan Inc, Tokyo).

RESULTS

PSYCHIATRIC STATES OF ABSTINENT METHAMPHETAMINE ABUSERS

Methamphetamine abusers showed no apparent negative symptoms as demonstrated by Brief Psychiatric Rating Scale assessment (Table 1). All methamphetamine abusers had previously experienced psychosis during methamphetamine use. Two methamphetamine abusers had persistent psychotic symptoms, such as persecutory delusions and auditory hallucinations; 5 had a depressed mood; 4 had anxiety; 4 showed severe aggression; and 4 had no psychiatric symptoms except for aggressive behavior. The mean AQ score was significantly higher in methamphetamine abusers than in controls ($t=-11.1$; $P<.001$).

ROI ANALYSIS

The traditional ROI-based analysis showed that methamphetamine abusers had significantly decreased [^{11}C](+)McN-5652 DVs in their global brain regions compared with control subjects (Wilks $\Lambda=0.001$; $P=.003$) (**Figure 2**). Subsequent univariate analysis of variance revealed that methamphetamine abusers had significantly lower [^{11}C](+)McN-5652 DVs than control subjects in all 10 ROIs studied ($P<.001$ for all). There was no group × sex interaction effect in the [^{11}C](+)McN-5652 DV, indicating no sex-specific effect in [^{11}C](+) McN-5652 DVs (Wilks $\Lambda=0.47$; $P=.37$).

Figure 3 shows the correlations between [^{11}C](+) McN-5652 DVs and clinical variables in methamphetamine abusers. The [^{11}C](+)McN-5652 DVs in 5 of the 10 ROIs (ie, the midbrain, thalamus, caudate nucleus, putamen, and orbitofrontal cortex) significantly correlated negatively with the duration of methamphetamine use ($P<.005$ for all by Pearson correlation coefficient) (Figure 3A). There was no correlation in any of the 10 ROIs between [^{11}C](+)McN-5652 DVs and the duration of methamphetamine abstinence, which lasted 6 months to 5 years in our participants (Figure 3B). The magnitude of aggression, as assessed using the AQ, increased significantly with decreasing [^{11}C](+)McN-5652 DVs in 8 of the 10 ROIs (ie, the thalamus, caudate nucleus, putamen, anterior cingulate cortex, temporal cortex, orbitofrontal cortex, dorsolateral prefrontal cortex, and cerebellar cortex) ($P<.005$ for all by Pearson correlation coefficient) (Figure 3C). Other clinical variables, including craving, were not statistically significantly correlated with changes in [^{11}C](+) McN-5652 DVs (data not shown).

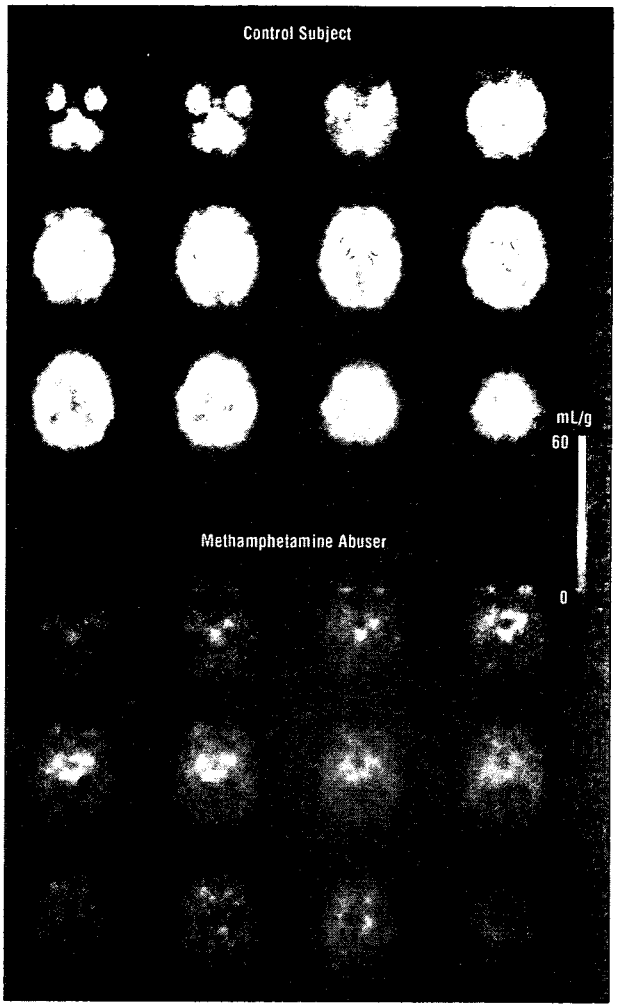

Figure 1. Voxel-based *trans*-1,2,3,5,6,10-beta-hexahydro-6-[4-(methylthio) phenyl]pyrrolo-[2,1-a]isoquinoline ([^{11}C](+)McN-5652) distribution volume images from a control subject and a methamphetamine abuser. These absolute parametric images were normalized to the standard stereotaxic brain atlas using transformation parameters for early integrated images of [^{11}C](+)McN-5652 (0-20 minutes after injection). The [^{11}C](+)McN-5652 distribution volumes in broad areas of the brain of the methamphetamine abuser were lower than those of the control subject.

SPM ANALYSIS

Figure 4 illustrates the results of the whole-brain voxel-based SPM analysis of [^{11}C](+)McN-5652 DVs. Figure 4A shows that the methamphetamine group had widely distributed reductions in [^{11}C](+)McN-5652 DVs compared with the control group ($P<.05$, corrected) (**Table 2**). In accord with the findings derived from the ROI analysis, the SPM analysis revealed an extensive clus-

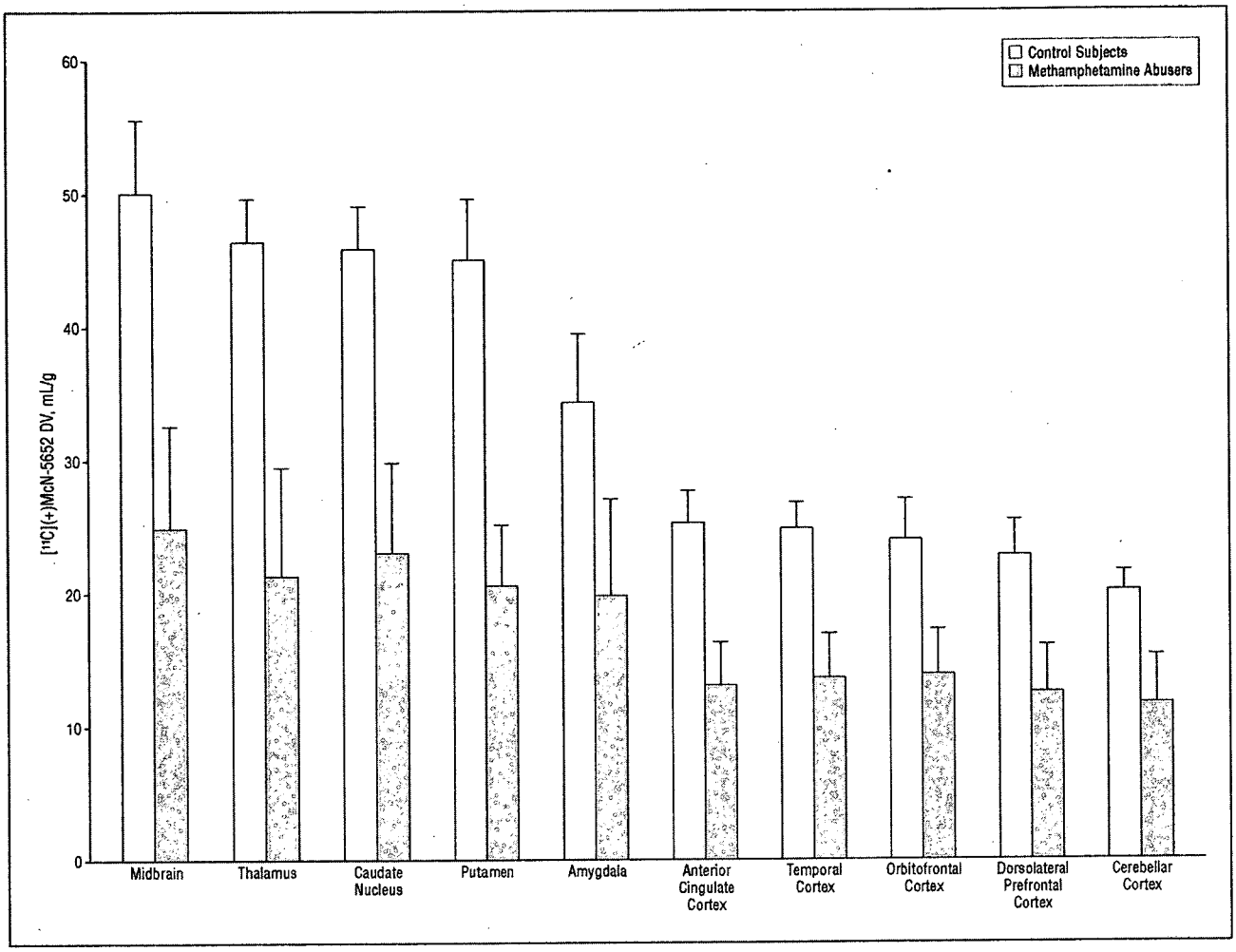

Figure 2. Mean regional brain *trans*-1,2,3,5,6,10-beta-hexahydro-6-[4-(methylthio)phenyl]pyrrolo-[2,1-a]isoquinoline ([^{11}C](+)McN-5652) distribution volumes (DVs) in control subjects and methamphetamine abusers. Methamphetamine abusers had significantly decreased [^{11}C](+)McN-5652 DVs in the global regions compared with controls (Wilks $\Lambda = 0.001$; $P = .003$, by multivariate analysis of variance). Univariate analysis of variance revealed that methamphetamine users had significantly lower [^{11}C](+)McN-5652 DVs than controls in all regions studied ($P < .001$ for all). Error bars represent SE.

ter of voxels with reduced [^{11}C](+)McN-5652 DVs occupying the right insular area and extending out into the bilateral putamen, caudate, thalamus, hypothalamus, midbrain, temporal, parietal, frontal, occipital, cerebellar, anterior cingulate, and posterior cingulate areas. This cluster consisted of 45 315 voxels (363 mL). Figure 4B shows clusters in which the magnitude of aggression increased significantly with decreasing [^{11}C](+)McN-5652 DVs. These clusters were located on the bilateral orbitofrontal areas ($P \leq .001$), left inferior temporal area ($P < .001$), and right anterior cingulate gyrus area ($P < .001$) (**Table 3**). The other clinical variables did not reach statistical significance (data not shown).

COMMENT

In the present study, methamphetamine abusers had statistically significantly decreased [^{11}C](+)McN-5652 DVs, a representative measure of serotonin transporter density,[21,39,44] in their global brain regions compared with control subjects. The finding of significantly reduced [^{11}C](+)McN-5652 DVs in a several brain regions in methamphetamine abusers, as revealed using the ROI approach, was in accord with the results of voxel-based SPM analysis. In addition, there was no group × sex interaction effect in terms of the [^{11}C](+)McN-5652 DV, indicating that abnormal [^{11}C](+)McN-5652 DVs in the brains of methamphetamine abusers are observed in both sexes. These findings suggest that the ingestion of methamphetamine leads to a global and severe reduction in the density of human brain serotonin transporters.

The values of the density of serotonin transporters in widely distributed brain regions, including the midbrain, hypothalamus, thalamus, caudate, putamen, amygdala, temporal cortex, and occipital cortex, were found to negatively correlate with the duration of methamphetamine use. This result implies that the longer methamphetamine is used, the more severe the decrease in serotonin transporter density will be. Although the duration of methamphetamine use is viewed as a proxy measure for the actual amount of intake of the drug, such a relationship in a dose-response manner strongly suggests a link between the use of methamphetamine and damage to serotonin neurons. This is compatible with the results of animal experiments[51] demonstrating dose-dependent methamphetamine-induced serotonin transporter reduction.

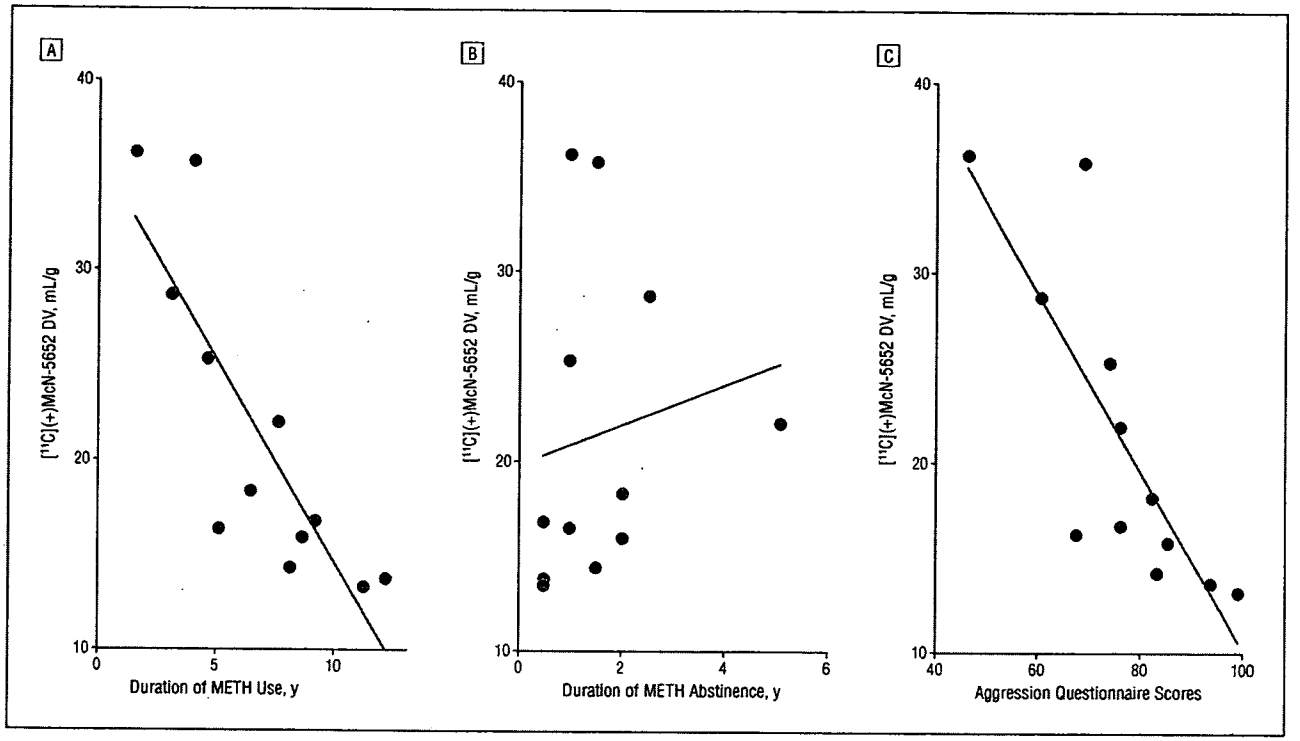

Figure 3. Correlations between *trans*-1,2,3,5,6,10-beta-hexahydro-6-[4-(methylthio)phenyl]pyrrolo-[2,1-a]isoquinoline ([^{11}C](+)McN-5652) distribution volumes (DVs) in a representative brain region (the thalamus) and clinical variables in methamphetamine (METH) abusers. A, Significant negative correlation between [^{11}C](+)McN-5652 DVs and the duration of METH use (r=–0.84; P=.001 by Pearson correlation coefficient). B, Correlation between [^{11}C](+)McN-5652 DVs and the duration of METH abstinence (r=0.16; P=.61). C, Correlation between Aggression Questionnaire scores and [^{11}C](+)McN-5652 DVs (r=–0.82; P=.001).

Although the present study was not designed to directly assess recovery from brain damage induced by methamphetamine use, there was no correlation between the [^{11}C](+)McN-5652 DVs and the duration of methamphetamine abstinence. Along with this finding, the result showing that even individuals who had been abstinent for more than 1 year (n=9) had a substantial decrease in serotonin transporter density (approximately a 30% decrease compared with controls) (Figure 3B) suggests that reductions in the density of the serotonin transporter in the brain associated with habitual methamphetamine abuse could persist long after methamphetamine use ceases.

The magnitude of aggression in methamphetamine abusers increased significantly with decreasing serotonin transporter densities in some brain regions. Detoxification from methamphetamine in all the abusers in this study was confirmed by regular urine drug screening as described in the "Drug Screening" subsection, including a test on the day of PET examination; these tests were conducted to establish that the psychiatric symptoms, such as aggression, were residual rather than acute symptoms induced by methamphetamine use. As a result, the relationship between the degree of aggressiveness and the density of serotonin transporter found in this study was not ascribed to the process of detoxification from methamphetamine use. Thus, the present findings indicate that methamphetamine-induced serotonergic disturbances are responsible for the elevated aggressiveness that is frequently observed, as a residual symptom, in abstinent methamphetamine abusers. This contention is consistent with a variety of studies[52,53] that have documented associations between decreased serotonergic function and increased aggression. For example, cerebrospinal fluid 5-hydroxyindoleacetic acid, which is known to reflect presynaptic serotonergic activity in the brain, has been found to be reduced in aggressive psychiatric patients,[54,55] impulsive violent men,[56,57] and impulsive violent offenders.[58]

In the correlational region analysis using SPM in the methamphetamine group, the magnitude of aggression was substantially associated with a decrease in serotonin transporter density in the clusters located in the orbitofrontal cortex, anterior cingulate, and temporal cortex, although the clusters were localized to small areas and did not fully occupy the anatomic brain regions. This result suggests that the potential methamphetamine-induced decrease in serotonergic function around these 3 areas may play an important role in the pathogenesis of elevated aggression in methamphetamine abusers. This is supported by several lines of evidence. For example, studies of brain injuries suggest that damage to the orbitofrontal and anterior cingulate areas produces syndromes characterized by aggression and impulsivity.[52,59] Furthermore, recent PET and postmortem clinicopathologic correlation studies have indicated that low levels of serotonin$_{1A}$ receptors in the orbitofrontal, anterior cingulate gyrus, and temporal areas are related to aggressive behavior.[60,61]

However, we cannot rule out the possibility that the increased aggression observed in methamphetamine abusers could reflect a preexisting condition, for example, an "addictive personality," which might often involve a tendency toward aggression.[62] Nevertheless, in the present study, we selected methamphetamine abusers who had no history of abnormal aggression before the use of meth-

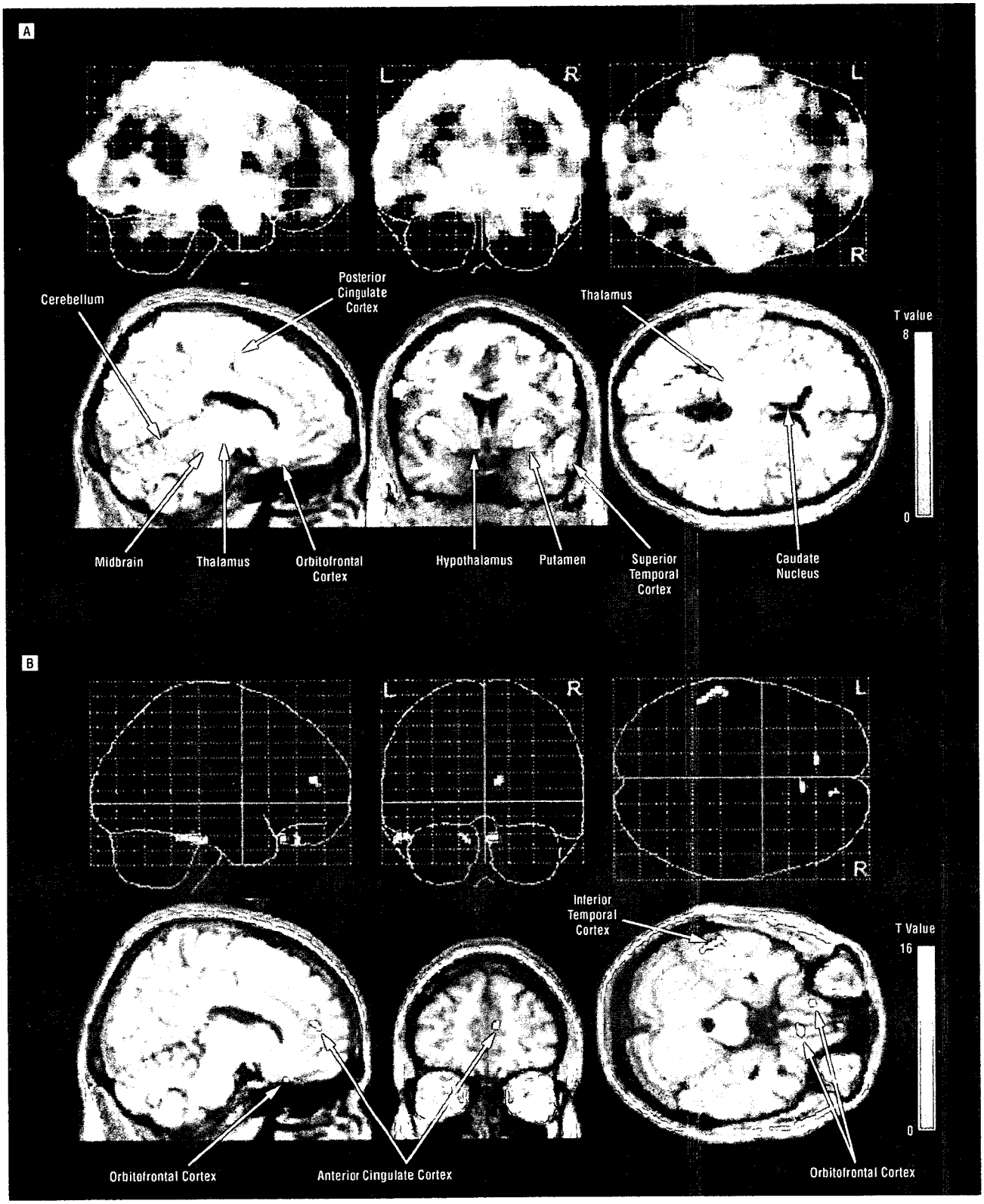

Figure 4. Results of the whole-brain voxel-based statistical parametric mapping analysis of the *trans*-1,2,3,5,6,10-beta-hexahydro-6-[4-(methylthio) phenyl]pyrrolo-[2,1-a]isoquinoline ([^{11}C](+)McN-5652) distribution volumes (DVs). A, Locations of methamphetamine abuser and control differences in [^{11}C](+)McN-5652 DVs. Areas with significantly reduced [^{11}C](+)McN-5652 DVs in methamphetamine abusers compared with those in controls ($P<.001$, corrected for cluster level) are given in Table 2. B, Locations of clusters with significant negative correlations between Aggression Questionnaire scores and [^{11}C](+)McN-5652 DVs in methamphetamine abusers ($P<.05$, corrected for voxel level) (Table 3). Each top row shows 3-dimensional glass brain views; each bottom row, detected area superimposed onto normal template magnetic resonance images.

amphetamine, and their histories were retrospectively confirmed by the abusers and their family members through detailed Structured Clinical Interview for *Diagnostic and Statistical Manual of Mental Disorders, Fourth Edition–*

Table 2. Voxel-Based Analysis of Regional Brain [^{11}C](+)McN-5652 Distribution Volume Reductions in 12 Methamphetamine Abusers Compared With 12 Control Subjects*

	Cluster-Level Analysis		Voxel-Level Analysis		Talairach Coordinates		
Location	Corrected *P* Value	Voxels, No.	Corrected *P* Value	*z* Score	x	y	z
Right insular cortex	<.001	45315	.009	5.33	34	13	-4
Left caudate nucleus	NA	NA	.02	5.12	-10	19	-4
Right claustrum	NA	NA	.03	5.02	32	0	-3

Abbreviations: [^{11}C](+)McN-5652, *trans*-1,2,3,5,6,10-beta-hexahydro-6-[4-(methylthio)phenyl]pyrrolo-[2,1-a]isoquinoline; NA, not available.
*The significance threshold was $P<.05$ at the corrected voxel level and $P<.05$ at the corrected cluster level. Coordinates are given in millimeters from the origin at the midpoint of the anterior commissure for voxels of peak significance.

Table 3. Voxel-Based Analysis of Regional Brain [^{11}C](+)McN-5652 Distribution Volumes Negatively Associated With Aggression Questionnaire Scores in 12 Methamphetamine Abusers*

	Cluster-Level Analysis		Voxel-Level Analysis		Talairach Coordinates		
Location	Corrected *P* Value	Voxels, No.	Corrected *P* Value	*z* Score	x	y	z
Right orbitofrontal cortex	<.001	20	.007	5.49	6	26	-21
Left inferior temporal cortex	<.001	38	.007	5.48	-57	-30	-19
Left orbitofrontal cortex	.001	10	.02	5.17	-10	34	-24
Right anterior cingulate cortex	<.001	12	.03	5.13	10	49	10

Abbreviation: [^{11}C](+)McN-5652, *trans*-1,2,3,5,6,10-beta-hexahydro-6-[4-(methylthio)phenyl]pyrrolo-[2,1-a]isoquinoline.
*The significance threshold was $P<.05$ at the corrected voxel level and $P<.05$ at the corrected cluster level. Coordinates are given in millimeters from the origin at the midpoint of the anterior commissure for voxels of peak significance.

based interviews. Furthermore, in this study, the severity of aggression clearly paralleled the decreases in serotonin transporter density in the brain, which in turn were found to be associated with the duration of methamphetamine use. Therefore, it seems unlikely that the increased aggression observed in these methamphetamine abusers reflected a preexisting disposition or personality trait.

Except for the scores on the AQ, none of the scores on the clinical rating scales for psychiatric symptoms were correlated with the decrease in serotonin transporter density. Methamphetamine has been reported to affect not only serotonergic neurons but also several other types of neurons, such as the dopaminergic, glutamatergic, and γ-aminobutyric acid (GABA)–ergic neurons, all of which have been implicated in the presence of a variety of psychiatric symptoms (eg, delusions, hallucinations, and anxiety).[63] It is possible that changes in various types of neurons might have affected or modified the clinical symptoms evaluated herein. Another plausible interpretation for the negative results is that, as seen in Table 1, the severity of most of the residual symptoms assessed in this study ranged from mild to moderate, and the variances of their distributions were relatively small; together, these factors may have biased the results toward the null hypothesis.

Herein, we recruited methamphetamine abusers from the community; they were recreational abusers of methamphetamine only, and none of them had used other illicit drugs or had taken toxic or high doses of methamphetamine. Although our strategy allowed us to evaluate the pure effects of methamphetamine on the human brain, the findings may not be generalized to the broad population of methamphetamine abusers. However, the combined use of methamphetamine with other illicit drugs is infrequent in Japan, as indicated by Japanese National Police Agency records in 2002.[64] One reason for this is that cannabis, cocaine, and major illicit drugs other than methamphetamine are not widely distributed in Japan.[64] Furthermore, a national survey of 233 methamphetamine abusers reported that only 2.6% of the abusers had undergone methamphetamine intoxication,[65] suggesting that abusers of an overdose of methamphetamine are rare in Japan. Consequently, our findings are considered to be fairly generalizable to the population of methamphetamine abusers, at least in Japan.

In this study, all the methamphetamine abusers exhibited some psychopathologic symptoms, even in an abstinent state. To our knowledge, no previous studies have examined the incidence of psychopathologic abnormalities in abstinent methamphetamine abusers recruited from the general community. In a study by Wada and Fukui,[65] who investigated the psychopathologic characteristics of 233 abstinent methamphetamine abusers recruited from hospitals in Japan (the period of abstinence exceeded 1 month; the mean ± SD duration of methamphetamine use was 11.1 ± 7.9 years), almost all the abusers exhibited some psychopathologic symptoms, such as auditory hallucinations, delusions of reference/persecution, mood disturbances, anxiety, insomnia, irritability, impulsivity, and personality changes, including the antisocial personality type. Such observations cannot be applied to absti-

nent abusers in the community as a whole but may provide some support for the high occurrence of psychopathologic symptoms observed in this study. In Japan, most methamphetamine abusers take the substance intravenously,[8] whereas in a study[66] from the United States, approximately 90% of methamphetamine abusers had no history of intravenous or intramuscular injection of methamphetamine. Furthermore, a study by Domier and colleagues[66] revealed that among recently abstinent methamphetamine abusers who had discontinued its use for several months, the injecting abusers had a significantly higher incidence of psychopathologic symptoms than the noninjecting abusers. These results suggest that in Japan, the intravenous intake of methamphetamine could predispose its abusers to persistent psychiatric problems, even after the cessation of methamphetamine use. Nevertheless, it remains an important and unresolved issue whether a reduction in serotonin transporter could be expected to occur in abusers with no psychopathologic signs or symptoms. To verify our findings that methamphetamine abuse is linked to a reduction in brain serotonin transporters, which in turn underlies persistent psychopathologic symptoms, additional studies that also incorporate a group of methamphetamine abusers with no apparent psychopathologic problems are required.

Wilson and colleagues[67] examined serotonin concentrations in postmortem tissue samples from human brains with a history of long-term methamphetamine abuse, although they did not study serotonin transporters per se. They concluded that there were no substantial alterations in serotonin concentrations in the global brain except in the medial prefrontal cortex (Brodmann area 11: a reduction of 56% compared with controls) and in the orbitofrontal cortex (Brodmann area 12: a reduction of 61% compared with controls). These results seem to contradict our observation of reductions in serotonin transporters in widely distributed brain regions. The discrepancy between the results of that postmortem study and those of present study is puzzling. However, one possible explanation for this discrepancy could be related to differences in the pattern and amount of drug use between the samples.[1,16,17] In Western countries, methamphetamine abusers often use other drugs, mainly cocaine or cannabis[68-70]; however, no information is provided with respect to this issue in the study by Wilson and colleagues.[67] Because methamphetamine is more likely to produce neurotoxic effects in serotonergic neurons than either cocaine or cannabis,[71,72] methamphetamine abusers who use this drug only could have experienced more severe damage to serotonergic neurons than abusers who simultaneously use other drugs, such as cocaine or cannabis. Furthermore, similar to most methamphetamine abusers in Japan, those in this study intravenously injected the substance. The intravenous intake may further potentiate the neurotoxic effects of methamphetamine.

To our knowledge, this is the first study to demonstrate a severe and long-lasting reduction in the density of the serotonin transporter in the living brains of methamphetamine abusers. The observed decrease in serotonin transporter density was also found to be associated with elevated levels of aggression. The present findings, combined with the results of previous animal studies, suggest that those who abuse methamphetamine may be at substantial risk for severe serotonin neuronal damage in the brain, potentially leading to persistently elevated aggression, even in those in a currently abstinent state.

Submitted for Publication: September 21, 2004; final revision received April 30, 2005; accepted July 7, 2005.
Correspondence: Yoshimoto Sekine, MD, PhD, Department of Psychiatry and Neurology, Hamamatsu University School of Medicine, 1-20-1 Handayama, Hamamatsu, Shizuoka 431-3192 Japan (ysekine@hama-med.ac.jp).
Acknowledgment: This work was supported by a Grant-in-Aid for the Center of Excellence from the Ministry of Education, Culture, Sports, Science, and Technology, Tokyo, Japan; research grant 16A for nervous and mental disorders from the Ministry of Health, Labor, and Welfare, Tokyo; a grant for the research on serotonin from the Public Health Research Foundation/New Frontiers of Neurotransmitter Research, Tokyo; and the Stanley Foundation, Bethesda, Md.

REFERENCES

1. McCann UD, Wong DF, Yokoi F, Villemagne V, Dannals RF, Ricaurte GA. Reduced striatal dopamine transporter density in abstinent methamphetamine and methcathinone users: evidence from positron emission tomography studies with [^{11}C]WIN-35,428. *J Neurosci.* 1998;18:8417-8422.
2. Volkow ND, Chang L, Wang GJ, Fowler JS, Leonido-Yee M, Franceschi D, Sedler MJ, Gatley SJ, Hitzemann R, Ding YS, Logan J, Wong C, Miller EN. Association of dopamine transporter reduction with psychomotor impairment in methamphetamine abusers. *Am J Psychiatry.* 2001;158:377-382.
3. Sekine Y, Iyo M, Ouchi Y, Matsunaga T, Tsukada H, Okada H, Yoshikawa E, Futatsubashi M, Takei N, Mori N. Methamphetamine-related psychiatric symptoms and reduced brain dopamine transporters studied with PET. *Am J Psychiatry.* 2001;158:1206-1214.
4. Farrell M, Marsden J, Ali R, Ling W. Methamphetamine: drug use and psychoses becomes a major public health issue in the Asia Pacific region. *Addiction.* 2002;97:771-772.
5. Hall W, Hando J, Darke S, Ross J. Psychological morbidity and route of administration among amphetamine users in Sydney, Australia. *Addiction.* 1996;91:81-87.
6. London ED, Simon SL, Berman SM, Mandelkern MA, Lichtman AM, Bramen J, Shinn AK, Miotto K, Learn J, Dong Y, Matochik JA, Kurian V, Newton T, Woods R, Rawson R, Ling W. Mood disturbances and regional cerebral metabolic abnormalities in recently abstinent methamphetamine abusers. *Arch Gen Psychiatry.* 2004;61:73-84.
7. Seivewright N. Disorders relating to the use of amphetamine and cocaine. In: Gelder MG, Lopez-Ibor JJ, Andreasen N, eds. *New Oxford Textbook of Psychiatry.* New York, NY: Oxford University Press; 2000:531-534.
8. Konuma K. Use and abuse of amphetamines in Japan. In: Cho AK, Segal DS, eds. *Amphetamine and Its Analogs.* San Diego, Calif: Academic Press; 1994:415-435.
9. Sekine Y, Minabe Y, Kawai M, Suzuki K, Iyo M, Isoda H, Sakahara H, Ashby CR Jr, Takei N, Mori N. Metabolite alterations in basal ganglia associated with methamphetamine-related psychiatric symptoms: a proton MRS study. *Neuropsychopharmacology.* 2002;27:453-461.
10. Sato M, Chen CC, Akiyama K, Otsuki S. Acute exacerbation of paranoid psychotic state after long-term abstinence in patients with previous methamphetamine psychosis. *Biol Psychiatry.* 1983;18:429-440.
11. Ricaurte GA, Schuster CR, Seiden LS. Long-term effects of repeated methylamphetamine administration on dopamine and serotonin neurons in the rat brain: a regional study. *Brain Res.* 1980;193:153-163.
12. Davidson C, Gow AJ, Lee TH, Ellinwood EH. Methamphetamine neurotoxicity: necrotic and apoptotic mechanisms and relevance to human abuse and treatment. *Brain Res Brain Res Rev.* 2001;36:1-22.
13. Matsuzaki H, Namikawa K, Kiyama H, Mori N, Sato K. Brain-derived neurotrophic factor rescues neuronal death induced by methamphetamine. *Biol Psychiatry.* 2004;55:52-60.

14. Ricaurte GA, Sabol KE, Seiden LS. Functional consequences of neurotoxic amphetamine exposure. In: Cho AK, Segal DS, eds. *Amphetamine and Its Analogs*. San Diego, Calif: Academic Press; 1994:297-313.
15. Kita T, Wagner GC, Nakashima T. Current research on methamphetamine-induced neurotoxicity: animal models of monoamine disruption. *J Pharmacol Sci*. 2003;92:178-195.
16. Villemagne V, Yuan J, Wong DF, Dannals RF, Hatzidimitriou G, Mathews WB, Ravert HT, Musachio J, McCann UD, Ricaurte GA. Brain dopamine neurotoxicity in baboons treated with doses of methamphetamine comparable to those recreationally abused by humans: evidence from [^{11}C]WIN-35,428 positron emission tomography studies and direct in vitro determinations. *J Neurosci*. 1998; 18:419-427.
17. Volkow ND, Chang L, Wang GJ, Fowler JS, Franceschi D, Sedler M, Gatley SJ, Miller E, Hitzemann R, Ding YS, Logan J. Loss of dopamine transporters in methamphetamine abusers recovers with protracted abstinence. *J Neurosci*. 2001; 21:9414-9418.
18. Sekine Y, Minabe Y, Ouchi Y, Takei N, Iyo M, Nakamura K, Suzuki K, Tsukada H, Okada H, Yoshikawa E, Futatsubashi M, Mori N. Association of dopamine transporter loss in the orbitofrontal and dorsolateral prefrontal cortices with methamphetamine-related psychiatric symptoms. *Am J Psychiatry*. 2003;160:1699-1701.
19. McCann UD, Szabo Z, Scheffel U, Dannals RF, Ricaurte GA. Positron emission tomographic evidence of toxic effect of MDMA ("Ecstasy") on brain serotonin neurons in human beings. *Lancet*. 1998;352:1433-1437.
20. Reneman L, Lavalaye J, Schmand B, de Wolff FA, van den Brink W, den Heeten GJ, Booij J. Cortical serotonin transporter density and verbal memory in individuals who stopped using 3,4-methylenedioxymethamphetamine (MDMA or "ecstasy"): preliminary findings. *Arch Gen Psychiatry*. 2001;58:901-906.
21. Szabo Z, McCann UD, Wilson AA, Scheffel U, Owonikoko T, Mathews WB, Ravert HT, Hilton J, Dannals RF, Ricaurte GA. Comparison of (+)-(11)C-McN5652 and (11)C-DASB as serotonin transporter radioligands under various experimental conditions. *J Nucl Med*. 2002;43:678-692.
22. Semple DM, Ebmeier KP, Glabus MF, O'Carroll RE, Johnstone EC. Reduced in vivo binding to the serotonin transporter in the cerebral cortex of MDMA ("ecstasy") users. *Br J Psychiatry*. 1999;175:63-69.
23. Scheffel U, Szabo Z, Mathews WB, Finley PA, Yuan J, Callahan B, Hatzidimitriou G, Dannals RF, Ravert HT, Ricaurte GA. Fenfluramine-induced loss of serotonin transporters in baboon brain visualized with PET. *Synapse*. 1996;24:395-398.
24. Bengel D, Isaacs KR, Heils A, Lesch KP, Murphy DL. The appetite suppressant d-fenfluramine induces apoptosis in human serotonergic cells. *Neuroreport*. 1998; 9:2989-2993.
25. McCann UD, Yuan J, Ricaurte GA. Neurotoxic effects of +/-fenfluramine and phentermine, alone and in combination, on monoamine neurons in the mouse brain. *Synapse*. 1998;30:239-246.
26. Poole R, Brabbins C. Drug induced psychosis. *Br J Psychiatry*. 1996;168:135-138.
27. Takebayashi K, Sekine Y, Takei N, Minabe Y, Isoda H, Takeda H, Nishimura K, Nakamura K, Suzuki K, Iwata Y, Sakahara H, Mori N. Metabolite alterations in basal ganglia associated with psychiatric symptoms of abstinent toluene users: a proton MRS study. *Neuropsychopharmacology*. 2004;29:1019-1026.
28. American Psychiatric Association. *Diagnostic and Statistical Manual of Mental Disorders, Fourth Edition*. Washington, DC: American Psychiatric Press; 1994.
29. First MB, Spitzer RL, Gibbon M, Williams JBW. *Structured Clinical Interview for the Diagnostic and Statistical Manual of Mental Disorders, Fourth Edition, Patient Version*. Washington, DC: American Psychiatric Press; 1997.
30. Al-Dirbashi OY, Kuroda N, Wada M, Takahashi M, Nakashima K. Quantification of methamphetamine, amphetamine and enantiomers by semi-micro column HPLC with fluorescence detection; applications on abusers' single hair analyses. *Biomed Chromatogr*. 2000;14:293-300.
31. Buss AH, Perry M. The aggression questionnaire. *J Pers Soc Psychol*. 1992;63: 452-459.
32. Hamilton M. The assessment of anxiety states by rating. *Br J Med Psychol*. 1959; 32:50-55.
33. Hamilton M. Development of a rating scale for primary depressive illness. *Br J Soc Clin Psychol*. 1967;6:278-296.
34. Mohr P, Horacek J, Motlova L, Libiger J, Czobor P. Prolactin response to D-fenfluramine challenge test as a predictor of treatment response to haloperidol in acute schizophrenia. *Schizophr Res*. 1998;30:91-99.
35. Overall JE, Gorham DR. The Brief Psychiatric Rating Scale. *Psychol Rep*. 1962; 10:799-812.
36. Volkow ND, Wang GJ, Fischman MW, Foltin RW, Fowler JS, Abumrad NN, Vitkun S, Logan J, Gatley SJ, Pappas N, Hitzemann R, Shea CE. Relationship between subjective effects of cocaine and dopamine transporter occupancy. *Nature*. 1997;386:827-830.
37. Ouchi Y, Nobezawa S, Okada H, Yoshikawa E, Futatsubashi M, Kaneko M. Altered glucose metabolism in the hippocampal head in memory impairment. *Neurology*. 1998;51:136-142.
38. Watanabe M, Shimizu K, Omura T, Takahashi M, Kosugi T, Yoshikawa E, Sato N, Okada H, Yamashita T. A new high resolution PET scanner dedicated to brain research. *IEEE Trans Nucl Sci*. 2002;49:634-639.
39. Parsey RV, Kegeles LS, Hwang DR, Simpson N, Abi-Dargham A, Mawlawi O, Slifstein M, Van Heertum RL, Mann JJ, Laruelle M. In vivo quantification of brain serotonin transporters in humans using [^{11}C]McN 5652. *J Nucl Med*. 2000; 41:1465-1477.
40. Ouchi Y, Yoshikawa E, Okada H, Futatsubashi M, Sekine Y, Iyo M, Sakamoto M. Alterations in binding site density of dopamine transporter in the striatum, orbitofrontal cortex, and amygdala in early Parkinson's disease: compartment analysis for β-CFT binding with positron emission tomography. *Ann Neurol*. 1999; 45:601-610.
41. Brody AL, Mandelkern MA, London ED, Childress AR, Lee GS, Bota RG, Ho ML, Saxena S, Baxter LR Jr, Madsen D, Jarvik ME. Brain metabolic changes during cigarette craving. *Arch Gen Psychiatry*. 2002;59:1162-1172.
42. Ouchi Y, Nobezawa S, Yoshikawa E, Futatsubashi M, Kanno T, Okada H, Torizuka T, Nakayama T, Tanaka K. Postural effects on brain hemodynamics in unilateral cerebral artery occlusive disease: a positron emission tomography study. *J Cereb Blood Flow Metab*. 2001;21:1058-1066.
43. Ouchi Y, Okada H, Yoshikawa E, Futatsubashi M, Nobezawa S. Absolute changes in regional cerebral blood flow in association with upright posture in humans: an orthostatic PET study. *J Nucl Med*. 2001;42:707-712.
44. Simpson HB, Lombardo I, Slifstein M, Huang HY, Hwang DR, Abi-Dargham A, Liebowitz MR, Laruelle M. Serotonin transporters in obsessive-compulsive disorder: a positron emission tomography study with [^{11}C]McN 5652. *Biol Psychiatry*. 2003;54:1414-1421.
45. Mikolajczyk K, Szabatin M, Rudnicki P, Grodzki M, Burger CA. JAVA environment for medical image data analysis: initial application for brain PET quantitation. *Med Inform (Lond)*. 1998;23:207-214.
46. Tauscher J, Kapur S, Verhoeff NP, Hussey DF, Daskalakis ZJ, Tauscher-Wisniewski S, Wilson AA, Houle S, Kasper S, Zipursky RB. Brain serotonin 5-HT (1A) receptor binding in schizophrenia measured by positron emission tomography and [^{11}C]WAY-100635. *Arch Gen Psychiatry*. 2002;59:514-520.
47. Talairach J, Tournoux P. *Co-planer Stereotaxic Atlas of the Human Brain: 3-Dimensional Proportional System: An Approach to Cerebral Imaging*. Stuttgart, Germany: Georg Thieme; 1988.
48. Ito K, Morrish PK, Rakshi JS, Uema T, Ashburner J, Bailey DL, Friston KJ, Brooks DJ. Statistical parametric mapping with ^{18}F-dopa PET shows bilaterally reduced striatal and nigral dopaminergic function in early Parkinson's disease. *J Neurol Neurosurg Psychiatry*. 1999;66:754-758.
49. Ouchi Y, Kanno T, Okada H, Yoshikawa E, Futatsubashi M, Nobezawa S, Torizuka T, Tanaka K. Changes in dopamine availability in the nigrostriatal and mesocortical dopaminergic systems by gait in Parkinson's disease. *Brain*. 2001; 124:784-792.
50. Wang GJ, Volkow ND, Chang L, Miller E, Sedler M, Hitzemann R, Zhu W, Logan J, Ma Y, Fowler JS. Partial recovery of brain metabolism in methamphetamine abusers after protracted abstinence. *Am J Psychiatry*. 2004;161:242-248.
51. Kovachich GB, Aronson CE, Brunswick DJ. Effects of high-dose methamphetamine administration on serotonin uptake sites in rat brain measured using [^{3}H]cyanoimipramine autoradiography. *Brain Res*. 1989;505:123-129.
52. Davidson RJ, Putnam KM, Larson CL. Dysfunction in the neural circuitry of emotion regulation: a possible prelude to violence. *Science*. 2000;289:591-594.
53. Coccaro EF, Kavoussi RJ, Hauger RL, Cooper TB, Ferris CF. Cerebrospinal fluid vasopressin levels: correlates with aggression and serotonin function in personality-disordered subjects. *Arch Gen Psychiatry*. 1998;55:708-714.
54. Coccaro EF. Central serotonin and impulsive aggression. *Br J Psychiatry Suppl*. 1989;8:52-62.
55. Virkkunen M, Rawlings R, Tokola R, Poland RE, Guidotti A, Nemeroff C, Bissette G, Kalogeras K, Karonen SL, Linnoila M. CSF biochemistries, glucose metabolism, and diurnal activity rhythms in alcoholic, violent offenders, fire setters, and healthy volunteers. *Arch Gen Psychiatry*. 1994;51:20-27.
56. Linnoila M, DeJong J, Virkkunen M. Monoamines, glucose metabolism, and impulse control. *Psychopharmacol Bull*. 1989;25:404-406.
57. Roy A, Adinoff B, Linnoila M. Acting out hostility in normal volunteers: negative correlation with levels of 5HIAA in cerebrospinal fluid. *Psychiatry Res*. 1988; 24:187-194.
58. Linnoila M, Virkkunen M, Scheinin M, Nuutila A, Rimon R, Goodwin FK. Low cerebrospinal fluid 5-hydroxyindoleacetic acid concentration differentiates impulsive from nonimpulsive violent behavior. *Life Sci*. 1983;33:2609-2614.
59. Grafman J, Schwab K, Warden D, Pridgen A, Brown HR, Salazar AM. Frontal lobe injuries, violence, and aggression: a report of the Vietnam Head Injury Study. *Neurology*. 1996;46:1231-1238.
60. Parsey RV, Oquendo MA, Simpson NR, Ogden RT, Van Heertum R, Arango V, Mann JJ. Effects of sex, age, and aggressive traits in man on brain serotonin

5-HT_{1A} receptor binding potential measured by PET using [C-11]WAY-100635. *Brain Res.* 2002;954:173-182.
61. Lai MK, Tsang SW, Francis PT, Esiri MM, Keene J, Hope T, Chen CP. Reduced serotonin 5-HT_{1A} receptor binding in the temporal cortex correlates with aggressive behavior in Alzheimer disease. *Brain Res.* 2003;974:82-87.
62. van den Bree MB, Svikis DS, Pickens RW. Genetic influences in antisocial personality and drug use disorders. *Drug Alcohol Depend.* 1998;49:177-187.
63. Wrona MZ, Yang Z, Zhang F, Dryhurst G. Potential new insights into the molecular mechanisms of methamphetamine-induced neurodegeneration. *NIDA Res Monogr.* 1997;173:146-174.
64. National Police Agency (Japan). *Criminal White Paper* [in Japanese]. Tokyo, Japan: Printing Bureau, Ministry of Finance of Japan; 2004.
65. Wada K, Fukui S. Relationship between years of methamphetamine use and symptoms of methamphetamine psychosis [in Japanese]. *Arukoru Kenkyuto Yakubutsu Ison.* 1990;25:143-158.
66. Domier CP, Simon SL, Rawson RA, Huber A, Ling W. A comparison of injecting and noninjecting methamphetamine users. *J Psychoactive Drugs.* 2000;32:229-232.
67. Wilson JM, Kalasinsky KS, Levey AI, Bergeron C, Reiber G, Anthony RM, Schmunk GA, Shannak K, Haycock JW, Kish SJ. Striatal dopamine nerve terminal markers in human, chronic methamphetamine users. *Nat Med.* 1996;2:699-703.
68. Richter KP, Ahluwalia HK, Mosier MC, Nazir N, Ahluwalia JS. A population-based study of cigarette smoking among illicit drug users in the United States. *Addiction.* 2002;97:861-869.
69. Sumnall HR, Wagstaff GF, Cole JC. Self-reported psychopathology in polydrug users. *J Psychopharmacol.* 2004;18:75-82.
70. Smart RG, Mann RE, Tyson LA. Drugs and violence among Ontario students. *J Psychoactive Drugs.* 1997;29:369-373.
71. Jacobsen LK, Staley JK, Malison RT, Zoghbi SS, Seibyl JP, Kosten TR, Innis RB. Elevated central serotonin transporter binding availability in acutely abstinent cocaine-dependent patients. *Am J Psychiatry.* 2000;157:1134-1140.
72. Croft RJ, Klugman A, Baldeweg T, Gruzelier JH. Electrophysiological evidence of serotonergic impairment in long-term MDMA ("ecstasy") users. *Am J Psychiatry.* 2001;158:1687-1692.

Clinical Trials Registration

In concert with the International Committee of Medical Journal Editors, *Archives of General Psychiatry* will require, as a condition of consideration for publication, registration of clinical trials in a public trials registry (such as http://ClinicalTrials.gov or http://controlled-trials.com). Trials must be registered at or before the onset of patient enrollment. This policy applies to any clinical trial starting enrollment after March 1, 2006. For trials that began enrollment before this date, registration will be required by June 1, 2006. The trial registration number should be supplied at the time of submission.

For details about this new policy see the editorials by DeAngelis et al in the September 8, 2004 (2004;292:1363-1364) and June 15, 2005(2005;293:2927-2929) issues of *JAMA*.

ELSEVIER

NeuroImage

www.elsevier.com/locate/ynimg
NeuroImage 29 (2006) 697 – 705

Cerebral hemodynamics evaluation by near-infrared time-resolved spectroscopy: Correlation with simultaneous positron emission tomography measurements

Etsuko Ohmae,[a,*] Yasuomi Ouchi,[b] Motoki Oda,[a] Toshihiko Suzuki,[a] Shuji Nobesawa,[b] Toshihiko Kanno,[b] Etsuji Yoshikawa,[a] Masami Futatsubashi,[a] Yukio Ueda,[a] Hiroyuki Okada,[a] and Yutaka Yamashita[a]

[a]*Central Research Laboratory, Hamamatsu Photonics K.K., 5000 Hirakuchi, Hamamatsu, Shizuoka 434-8601, Japan*
[b]*Positron Medical Center, Hamamatsu Medical Center, 5000 Hirakuchi, Hamamatsu, Shizuoka 434-0041, Japan*

Received 18 August 2004; revised 3 March 2005; accepted 4 August 2005
Available online 13 September 2005

We compared pharmacologically-perturbed hemodynamic parameters (cerebral blood volume; CBV, and flow; CBF) by acetazolamide administration in six healthy human subjects studied with positron emission tomography (PET) and near-infrared (NIR) time-resolved spectroscopy (TRS) simultaneously to investigate whether NIR-TRS could measure in vivo hemodynamics in the brain tissue quantitatively. Simultaneously with the PET measurements, TRS measurements were performed at the forehead with four different optode spacing from 2 cm to 5 cm. Total hemoglobin and oxygen saturation (SO_2) measured by TRS significantly increased after administration of acetazolamide at any optode spacing in all subjects. In PET study, CBV and CBF were estimated in the following three volumes of interest (VOIs) determined on magnetic resonance images, VOI_1: scalp and skull, VOI_2: gray matter region, VOI_3: gray and white matter regions. Acetazolamide treatment elevated CBF and CBV significantly in VOI_2 and VOI_3 but VOI_1. TRS-derived CBV was more strongly correlated with PET-derived counterpart in VOI_2 and VOI_3 when the optode spacing was above 4 cm, although optical signal from cerebral tissue could be caught with any optode spacing. As to increase of the CBV, 4 cm of optode spacing correlated best with VOI_2. To support the result of TRS-PET experiment, we also estimated the contribution ratios of intracerebral tissue to observed absorption change based on diffusion theory. The contribution ratios at 4 cm were estimated as follows: 761 nm: 50%, 791 nm: 72%, 836 nm: 70%. These results demonstrated that NIR-TRS with 4 cm of optode spacing could measure cerebral hemodynamic responses optimally and quantitatively.

Introduction

Near-infrared spectroscopy (NIRS) allows simple, non-invasive measurement of the oxygenation state and hemodynamics in living tissue by utilizing the differential in absorption spectrum between oxygenated and deoxygenated hemoglobin. This field got its start from the finding by Jobsis (1977) that when a cat's head is irradiated with near-infrared (NIR) light, the intensity of the transmitted light shows changes according to the oxygen metabolic state in the tissues. Since then, there has been growing study and technique of NIRS measurement.

Making that advantage, this method has been expected for use in surgical operations (Kakihana et al., 1996; De Blasi et al., 1997) and neonate respiration care (Meek et al., 1999; Isobe et al., 2000). Besides the clinical field, topographical imaging by multi-channels measurement is being performed to observe brain activity on the cortex (Watanabe et al., 2000; Tanosaki et al., 2001).

NIRS encompasses some different techniques and analysis, and we are adopting approaches of time-resolved spectroscopy (TRS; Oda et al., 1996; Yamashita et al., 1998), phase modulated spectroscopy (PMS; Tuchiya and Urakami, 1996; Iwai et al., 2001) or spatially resolves spectroscopy (SRS; Suzuki et al., 1999) method, etc. to quantification.

In contrast to the wide applicability of NIRS to brain monitoring, fundamental and critical questions still remain to be clarified, one of which is light propagation in the human head. The effect of the various external tissues of the head such as skin, skull and cerebrospinal fluid (CSF) on photon propagation in the internal cerebral tissue has not yet been fully examined in vivo.

Several researchers (Firbank et al., 1995; Okada et al., 1997) expressed doubts about the use of NIRS on adult human heads due to problems from the multi-layered structure of the scalp, skull, CSF and the cerebral tissue. Firbank first showed that the presence of CSF had a significant effect on the light distribution. It was

* Corresponding author. Fax: +81 53 586 6180.
E-mail address: etuko-o@crl.hpk.co.jp (E. Ohmae).
Available online on ScienceDirect (www.sciencedirect.com).

1053-8119/$ - see front matter © 2005 Elsevier Inc. All rights reserved.
doi:10.1016/j.neuroimage.2005.08.008

reported that the NIRS signal from the adult human head was only 10–20% of the total signal due to the effect of CSF from the Monte Carlo simulation. These doubts are related to the essential question of where to measure using the photon, and research studies are being conducted using both simulations (Okada and Delpy, 2000, 2003a,b; Misonoo and Okada, 2001) and experimental measurements. On the contrary, several researchers (McCormick et al., 1992; Harris et al., 1994; Germon et al., 1995; Kohri et al., 2001) have reported that NIRS can detect the brain signals more specifically by increasing the optode spacing from experimental measurements.

In this study, in order to investigate the relation between the optode spacing and light sampling depth, we observed change in the cerebral blood volume (CBV) of six adult subjects by administration of a drug with simultaneous measurement of the TRS system which can measure the blood volume and the oxygen saturation (SO_2) quantitatively and positron emission tomography (PET), and we compared the CBV by TRS (TRS CBV) with CBV by PET (PET CBV) and estimated the contribution ratios of intracerebral tissue to the observed absorption change at three different wavelengths.

Materials and methods

Subjects

Six healthy male subjects (mean age, 42.6 ± 5.08; range, 37 to 51 years) were studied. Informed consent was obtained from all subjects before experiment. It was confirmed that they had no previous history of intracranial disorders and also that there were no anatomical abnormalities by making a check with a magnetic resonance imaging (MRI; 0.3 T MRP7000AD, Hitachi Ltd., Japan).

Three-wavelength TRS system

We used TRS-10 system (Hamamatsu Photonics K.K., Japan) (Oda et al., 2000) to obtain TRS-CBV in our experiment. This system uses time-correlate single photon counting (TCPC) method for measuring the temporal function of the sample. The system measures the intensity of light in a time domain and enables analysis of to the data with the time domain photo diffusion equation (Patterson et al., 1989). The block diagram of this system is shown in Fig. 1.

As the light source, this system uses semiconductor lasers called "Picosecond Light Pulser (PLP, Hamamatsu Photonics K.K., Japan)" emitting light pulses at three different wavelengths (761 nm, 791 nm, 836 nm) with a peak power of 60 mW, average power of 30 μW, the full with at half maximum (FMHM) of 100 ps and repetition frequency of 5 MHz. The detector section of this system consists of a photomultiplier tube (PMT, H6279-MOD, Hamamatsu Photonics K.K., Japan) followed by constant fraction discriminators (CFD), time-to-amplitude converters (TAC), A/D converters and histogram memories.

The system instrumental function is about 160 ps FMWH. The three PLPs emit light pulses on a time series, and the 3-wavelength optical pulses (761, 791, 836 nm) are guided into one optical fiber via a fiber coupler (CH20G-D3-CF, Mitsubishi Gas Chemical Company Inc., Japan). An optical switch (SC SERIES, JDS FITEL Inc., Canada) in this experiment selected the light irradiation point. A neutral density filter installed between the optical switch and each irradiation fiber maintained the light entering the PMT at a correct level. Each single optical fiber (GC200/250L, FUJIKURA Ltd., Japan) used for light irradiation has a numerical aperture (N.A.) of 0.25 and a core diameter of 200 μm. The optical bundle fiber (LB21E, HOYA Corp., Japan) used to collect the light has an N.A. of 0.21 and a bundle diameter of 3 mm.

TRS data analysis

The observed temporal profiles were fitted into the photon diffusion equation (Patterson et al., 1989) using the non-linear least square fitting method. The reduced scattering (μ_s') and absorption coefficients (μ_a) for three wavelengths were calculated (Appendix A). Then oxyhemoglobin (TRS HbO_2), deoxyhemoglobin (TRS Hb), total hemoglobin (TRS tHb) and oxygen saturation (SO_2) were calculated with least square method (Appendix B). We then converted the TRS tHb into the TRS CBV for comparison with the PET CBV (Appendix C). Additionally, we calculated the partial mean pathlength of extracerebral tissue (L_{ext}) at each wavelength

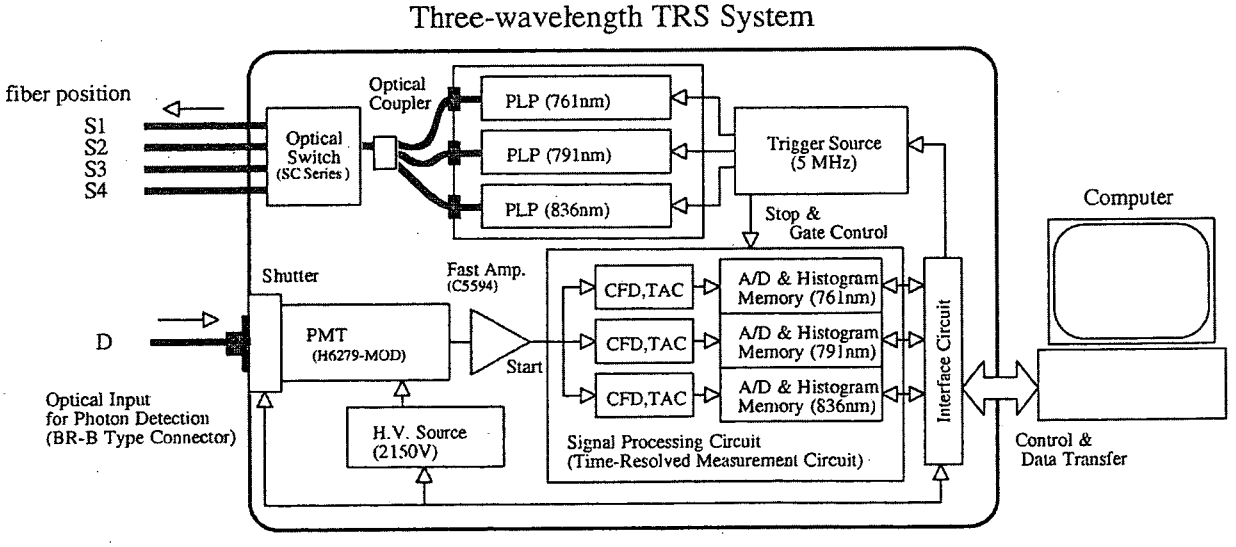

Fig. 1. Block diagram of time-resolved spectroscopy system (TRS-10: Hamamatsu Photonics K.K.).

by applying the method by the reference (Kohri et al., 2001) for five subjects whose absorption coefficients (μ_a) increased proportional to optode spacing from 2 to 4 cm. The observed mean pathlength (L_{obs}) was calculated (Zhang et al., 1998) from temporal profiles. Then, we determined the contribution ratio of the intracerebral tissue to the observed absorption change using these values.

TRS fiber position

Prior to the experiment, headgear was made for each volunteer to fix the TRS optical fibers to their left forehead. The headgear was made of thermoplastic material (ESS-15, Engineering System Co., Japan) to ensure a secure fit onto the head of each volunteer. A total of five fiber holders were fabricated for four light irradiation points (S_{1-4}) with optode spacings of 2, 3, 4 and 5 cm and one light detection point (D), and a black sheet was affixed to the inner side of the headgear except for the fiber holders to shield a detection fiber from stray light propagating on the skin surface. More specifically, the light irradiation point S_4 was first established on the left forehead, at a point 35 mm above supra-orbital margin so as to avoid the frontal sinus, and also 1 cm away from the median line to avoid the superior sagittal sinus. Next, the other light irradiation and detection points (S_{1-3}, D) were established using this point (S_4) as a reference. The positions of the light irradiation and detection points (S_{1-4}, D) on the MRI image of the head are shown in Fig. 2A. After measurement was complete, the value of optode spacing for substitution into the photon diffusion equation was measured as a straight distance with calipers. Fabricating headgear allowed the measurement to be easily made and permitted setting accurate optode spacing.

PET procedure

PET was performed using a high resolution PET scanner (SHR22000, Hamamatsu Photonics KK, Hamamatsu, Japan) (Iwase et al., 2002) with spatial resolution of 3.6 mm at full width half maximum (FWHM) transaxially and 4.2 mm axially, and with a 23-cm axial field of view, yielding 63 image slices simultaneously. After backprojection and filtering, the image resolution was 8.0 × 8.0 × 5.3 mm FWHM. The voxel of each reconstructed image measured 1.73 × 1.73 × 3.6 mm. Just prior to PET measurement, each subject underwent an MRI for determining the brain scanning area by using a static magnet with 3-dimensional mode acquisition (Ouchi et al., 1998). Fifteen-minute transmission scan for attenuation correction was performed with a $^{68}Ge/^{68}Ga$ source.

We applied the ^{15}O-CO short inhalation method followed by 5 min of data acquisition to measure the PET CBV (Lammertsma and Jones, 1983; Lammertsma et al., 1987). During this acquisition period, two pairs of arterial blood samples were collected for determining arterial ^{15}O-CO radioactivity.

One hundred twenty-second dynamic emission scans (10 s × 12 frames) were performed while subjects received a 500-MBq bolus of $H_2^{15}O$ through the right cubital vein by an automated injector. Simultaneously after injection, arterial blood was continuously withdrawn through the left brachial artery using the automated arterial blood γ-ray coincidence counter (BACC-2: Hamamatsu Photonics K.K., Hamamatsu, Japan) yielding arterial input data per second (Ouchi et al., 2001). A quantitative PET CBF value was estimated using 2-min $H_2^{15}O$ data accumulated after the tracer started circulating in the brain by summing the dynamic frames based on the autoradiographic method (Herscovitch et al., 1983).

Physiological parameters were monitored during PET examination and additional arterial blood samples were taken after each scan for analyzing levels of $PaCO_2$, Hb, hematocrit and arterial pH using a blood gas analyzer (Bayer Rapidlab 860, Tokyo, Japan). The psychophysical condition of each subject was evaluated by asking if any different sensation or mental activity was developed during the whole measurement in order to exclude any change in such brain activities as a confounding factor.

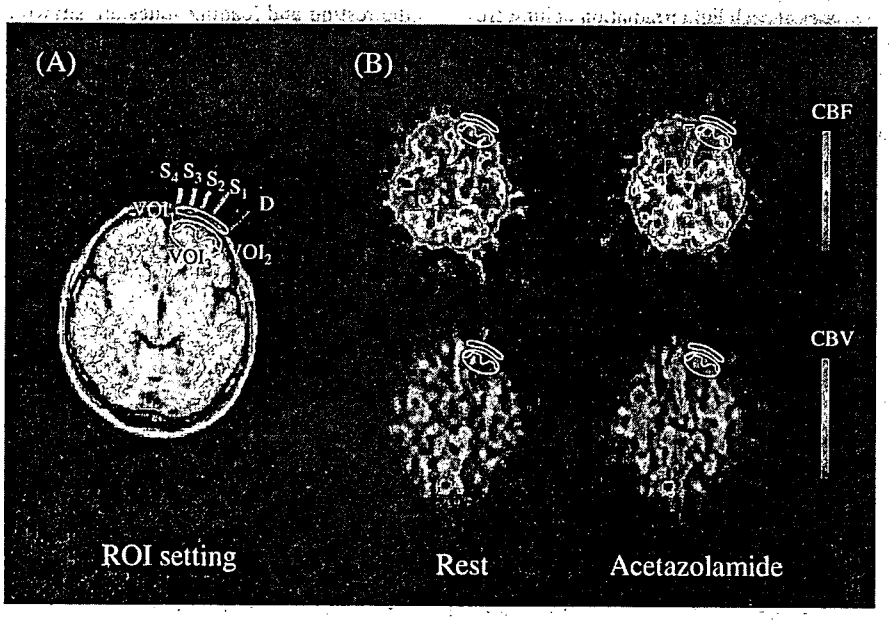

Fig. 2. Fiber and VOI positions setting on MRI image and PET images. (A) Fiber markers appear on left forehead. S_{1-4} and D are corresponding to irradiation fibers and a detection fiber, respectively. Optode spacings of S_1-D: 2 cm, S_2-D: 3 cm, S_3-D: 4 cm, S_4-D: 5 cm were set. The four PET VOIs were set as follows. VOI_1: extracerebral tissue, VOI_2: gray matter region, VOI_3: gray matter and white matter regions. (B) Images of typical measurements (41 years old; male) of PET CBF (upper) and PET CBV (lower) in the resting (left) and loading (right) state.

After measurements, to grasp the TRS light irradiation and detection points on the PET image, the fiber positions were marked by multi-modality radiographic markers (MM-3004, I.Z.I Medical Products Corp., USA) and the brain once again measured by MRI.

PET VOI

The volume of interest (VOI) on PET image used for comparison with TRS values was set by means of the following procedure. First of all, 3-dimensional MRI images were cut into 3.6 mm thick slices transversely along the multi-modality radiographic marker line. Then two slices involving these markers were selected from all these slices. Next, the following four VOIs were placed under S_4-D area on the two slices. These were set as VOI_1: extracerebral tissues (such as scalp and skull), VOI_2: gray matter region, VOI_3: gray matter and white matter regions. These VOIs were then repositioned on the PET image matching the selected two MRI slices as the PET VOIs. Mean values for each VOI size were VOI_1: 2.88 cm^3, VOI_2: 3.16 cm^3, VOI_3: 5.99 cm^3. The VOI settings are shown in Fig. 2A.

Since the PET CBF and PET CBV values were calculated with coefficients established for intracerebral tissues, the data of VOI_1 set in extracerebral tissues were treated with arbitrary unit.

Protocol

PET measurements were performed in the resting state (before administration) and the loading state (after administration) at more than 20 min after the intravenous administration of 1000 mg acetazolamide (Diamox, Japan Wyeth Ledele Ltd., Japan) appeared to be the maximum effect of cerebral vasodilatation. Two CBF measurements and one CBV measurement with PET were performed in resting and loading state.

In the TRS measurement, the optode spacings were changed in sequence by switching the four light irradiation points (S_{1-4}) with an optical switch. To maintain a peak count greater than 5000 (Suzuki et al., 1994), the acquisition times at each light irradiation point were set to 10, 20, 30 and 120 s. These TRS measurements were performed consecutively on a time series from the start to the finish of the PET measurements. Subjects were kept at rest while lying face up on the bed during measurements. The protocol is shown in Fig. 3.

Statistical analysis

All results were expressed as mean ± SD. Statistical significance of the changes in PET CBV, PET CBF, TRS CBV and SO_2 before and after administration of acetazolamide was analyzed by paired t test. Statistical significance of contribution ratio among wavelengths was analyzed by ANOVA and Bonferroni t test. A significant difference was defined when statistical probability: P was less than 0.05.

The association between TRS CBV and PET CBV was evaluated by squared Pearson's correlation coefficient (r^2). Change in CBV (ΔCBV) by administration of acetazolamide was also evaluated in the same way. The assessment for VOI_1 was not performed because it was expressed in the arbitrary unit. Statistical significance of r^2 was analyzed by a t test for r^2. A significant difference was defined when statistical probability: P was less than 0.05.

Results

Physiology

There were no significant changes in physiologic parameters (arterial blood pressure, pulse rates, $PaCO_2$) and psychophysical states (changes in mental activity) between before and after administration of acetazolamide (data is not shown).

TRS

Typical values of TRS tHb and SO_2 at each optode spacing during the experiment are shown in Fig. 4. The rise of TRS tHb and SO_2 was confirmed at all optode spacings immediately after administering acetazolamide and reached a plateau after about 10 min. These phenomena were observed in all subjects.

Mean values of TRS CBV and SO_2 at each optode spacing in the resting and loading states are shown in Fig. 5. The TRS CBV and SO_2 at each optode spacing in resting state were as follows: 2 cm: 2.7 ± 0.4 cm^3/100 g, 70.3 ± 1.1%, 3 cm: 3.0 ± 0.2 cm^3/100 g, 68.7 ± 1.8%, 4 cm: 3.0 ± 0.3 cm^3/100 g, 69.6 ± 2.3%, 5 cm: 2.7 ± 0.3 cm^3/100 g, 71.7 ± 2.8%. The TRS CBV and SO_2 in loading

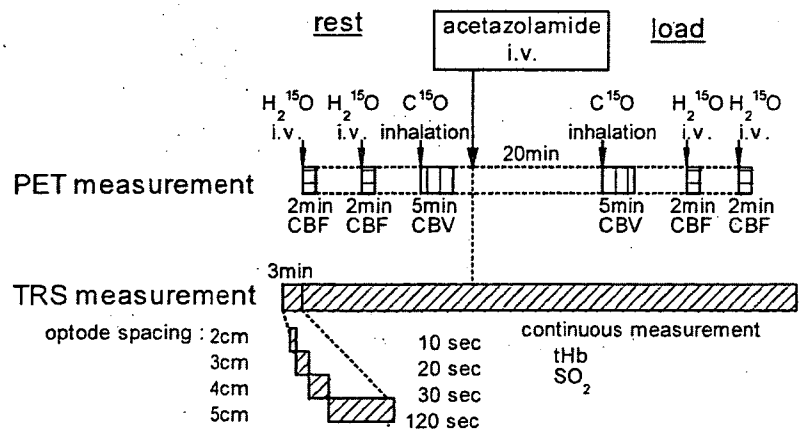

Fig. 3. TRS and PET simultaneous measurement protocol. The TRS measurement was made while switching the light irradiation point to set optode spacings of 2, 3, 4 and 5 cm. Data acquisition time was 10, 20, 30 and 120 s at each irradiation point. In the PET measurement, CBF was measured twice and CBV once, both resting and loading state. One CBF measurement required 2 min and the CBV measurement 5 min.